Supporting Information

Table of Contents

1. General Methods and Materials

All solvents were purified before use. Toluene was distilled from CaH_2. 1,1,3,3,5,5-Hexamethyltrisiloxane were purchased from ABCR and used without purifications. Platinum(0)-1,3-divinyl-1,1,3,3-tetramethyldisiloxane complex solution (in xylene, Pt-2%) was purchased from Sigma-Aldrich. The reactions were monitored by thin-layer chromatography (TLC) using Fluka silica gel (60 F 254) plates (0.25 mm). Visualization was made with UV light. IR spectra were obtained using an IR spectrometer with a Fourier transformer Bruker "Tensor 37" (Germany). The samples were prepared by pressing KBr pellets. ^{1}H, ^{13}C, ^{19}F and ^{29}Si NMR spectra were recorded on a Bruker Avance 300 (300 MHz; Germany), Bruker Avance 400 (400 MHz; Germany) spectrometer. Chemical shifts are reported relative to chloroform (δ=7.25 ppm) for ^{1}H NMR and chloroform (δ=77.00 ppm) for ^{13}C NMR. High-resolution mass spectra (HRMS) were measured using a Bruker micrOTOF II instrument with electrospray ionization (ESI) (Germany). The absorption spectra were recorded on a Shimadzu UV-1900 spectrophotometer (Japan). The fluorescence spectra were measured on the Agilent Cary Eclipse Fluorescence Spectrophotometer (USA). Spectroscopic grade solvents (Aldrich) were used in UV-vis absorption and fluorescence measurements. Fluorescence quantum yields were determined using fluorescein in 0.1 M NaOH in water and 9,10-diphenylanthracene in cyclohexane as a references and calculated by the following equation:

$$\Phi_{sample} = \Phi_{reference} \times \frac{I_{sample}}{I_{reference}} \times \frac{A_{reference}}{A_{sample}} \times \frac{n^2_{sample}}{n^2_{reference}},$$

where Φ is the QY, I is the integral intensity of the corrected fluorescence emission spectrum, A is the absorbance at the excitation wavelength, n is the refractive index of the solvent. Fluorescence decay curves were obtained with spectrofluorometer Fluotime 300 (Picoquant). LDH-D-C-375 was used as excitation source (λ_{ex}=375 nm). Data fitting was performed using Easytau2 (Picoquant) software. The program is using the following model for multiexponential fitting of experimental data:

$$\text{Dec}(t) = \left[\int_{-\infty}^{t} dt' \left[\text{IRF}(t - Shift_{IRF}) - Bkgr_{IRF} \right] \left[\sum_{i=1}^{n_{Exp}} A_i \, e^{-\frac{t-t'}{\tau_i}} \right] \right] + Bkgr_{Dec}$$

$$I_m = A_m \tau_m$$

FWHM of instrument response function (IRF) is about 180 ps and determines manly by detection system (laser pulse FWHM is about 40 ps). According to literature[1] estimation for exponential lifetimes in deconvolution procedure used is about 0.1 FWHW IRF the same estimation is proposed by equipment manufacturer. Thus, in our case lifetime accuracy is about 20 ps and this is upper estimation. More precise experimental estimation may be performed using the following method[2]. Two pump pulse profiles are measured, a length of time

corresponding to the time needed to collect an ordinary decay curve being allowed to elapse between the two measurements. Deconvolution of one pump pulse profile with the other will yield a "decay" time, which is a measure of the time resolution of the instrument. In our case error obtained using this method is about 6 ps with about 10 minutes between measurements.

To choose appropriative number of exponential terms we have used criteria that $\chi 2$ is in range 0.8 - 1.3[3] and uniformity of residuals distribution and auto-correlation function around zero. For example, results of bi-, tri- and four exponential fitting of decay curve obtained at 420 nm for **5 a** in cyclohexane is presented in figure S69 the corresponding autocorrelation functions are presented in figure S70.

Excitation energy transfer efficiency estimation

We have used three methods for estimation of excitation energy transfer efficiency Φ_{ET}. The detailed discussion on this topic can be found in literature[4]. In method 1 efficiency is estimated using fluorescence lifetimes of donor in dyad and free state according to formula:

$$\Phi_{ET}=k_{ET}\times\tau_{DA}=k_{ET}/(k_{ET}+1/\tau_D)=1-\tau_D/\tau_{DA}$$

where τ_{DA} – fluorescence lifetime of donor in dyad, τ_D – fluorescence lifetime of free donor, k_{ET} - rate constant of energy transfare.

In method 2 the same principle is utilized but donor fluorescence quantum yields are used for the calculations:

$$\Phi_{ET}=1-\tau_D/\tau_{DA}=1-(k_D{}^f\times\tau_D)/(k_D{}^f\times\tau_{DA})=1-\Phi_D/\Phi_{DA}$$

where Φ_{DA} – fluorescence quantum yield of donor in dyad, Φ_D – fluorescence quantum yield of free donor, $k_D{}^f$ – radiation rate constant of donor.

It is worth to note that these two methods relay on fact that quenching of donor in excited state is only due to the energy transfer. All excitation energy lost by donor will be received by acceptor. In general, it is not always valid assumption. To more precisely estimate Φ_{ET} let consider the following equation which describes integral fluorescence intensity of acceptor unit when the system is excited at donor wavelength 375nm. In this case fluorescence arises due to direct acceptor excitation and excitation through donor:

$$I_{375}=\Phi_{375}{}^{BODIPY}\times(D_{375}{}^{BODIPY}+D_{375}{}^{DBMBF2})\times I=\Phi_{475}{}^{BODIPY}\times(D_{375}{}^{BODIPY}+\Phi_{ET}\times D_{375}{}^{DBMBF2})\times I$$

where I – excitation light intensity, $\Phi_{375}{}^{BODIPY}$ – BODIPY unit quantum yield upon excitation at 375 nm, $\Phi_{475}{}^{BODIPY}$ – BODIPY unit quantum yield upon excitation at 475 nm, $D_{375}{}^{BODIPY}$ – optical density at 375 nm related to BODIPY unit, $\Phi_{375}{}^{DBMBF2}$ – optical density at 375 nm related to $DBMBF_2$ unit. From this equation the following equation for Φ_{ET} can be obtained.

$$\Phi_{ET}=(\Phi_{375}{}^{BODIPY}\times(D_{375}{}^{BODIPY}+D_{375}{}^{DBMBF2}))/(\Phi_{475}{}^{BODIPY}\times D_{375}{}^{DBMBF2})-D_{375}{}^{BODIPY}/D_{375}{}^{DBMBF2}=$$

$$(\Phi_{375}{}^{BODIPY}\times(\varepsilon_{375}{}^{BODIPY}+\varepsilon_{375}{}^{DBMBF2}))/(\Phi_{475}{}^{BODIPY}\times\varepsilon_{375}{}^{DBMBF2})-\varepsilon_{375}{}^{BODIPY}/\varepsilon_{375}{}^{DBMBF2}$$

2. Synthesis

*Allyl-DBMBF₂ (1 a).* It was synthesized by the method described earlier by us.[5]
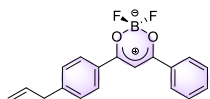
*Allyl-DBMBF₂-OCH₃ (1 b).* It was synthesized by the method described earlier by us.[6]
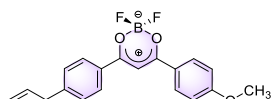
Meso-decene-BODIPY (4). It was synthesized by the method described earlier by us.[7]
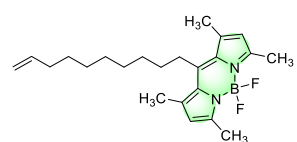
General method for synthesis of DBMBF₂-BODIPY dyads. (5 a,b).

A mixture of corresponding allyl-DBMBF₂ **1 a,b** (0.001 mol), 1,1,3,3,5,5-hexamethyltrisiloxane **2** (1.042 g, 0.005 mol) and Karstedt catalyst (30 µL) in dry toluene (20 mL) was stirred at room temperature for 24 h. After the reaction was complete a solvent and excess of **7** were removed by rotor evaporator and the residue was dried in vacuo. The obtained hydride siloxane derivative of DBMBF₂ **3 a,b** was used in the next step without purification. A mixture of hydride siloxane derivative of DBMBF₂ **3 a,b** (0.524 g, 0.001 mol), *meso*-decene-BODIPY **4** (0.384 g, 0.001 mol) and Karstedt catalyst (30 µL) in dry toluene (20 mL) was stirred at room temperature for 24 h. After the reaction was complete a solvent was removed by rotor evaporator. The residue was purified by flash chromatography on C18 silica with acetonitrile as an eluent. DBMBF₂-BODIPY dyads **5 a,b** were obtained as an orange oil.

DBMBF₂-BODIPY (5 a). **Yield**: 25 %. **¹H NMR** (300 MHz, CDCl₃): δ 0.02 (s, 6H, SiCH₃), 0.05 (s, 6H, SiCH₃), 0.08 (s, 6H, SiCH₃), 0.49-0.61 (m, 4H, SiCH₂), 1.27 (m, 12H, CH₂), 1.39-1.65 (m, 4H, CH₂), 1.67-1.74 (m, 2H, CH₂), 2.36 (s, 6H, CH₃), 2.48 (s, 6H, CH₃),
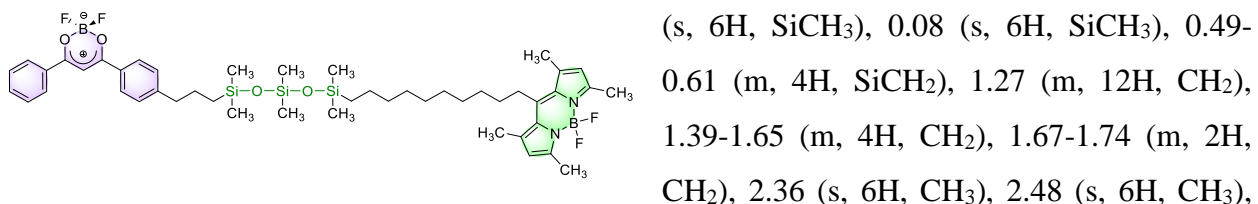
2.72 (t, 2H, *J*=7.3 Hz, CH₂), 2.86 (m, 2H, CH₂), 6.00 (s, 2H, BODIPY-CH), 7.16 (s, 1H, COCHCO), 7.32 (d, 2H, *J*=7.9 Hz, Ar), 7.51 (t, 2H, *J*=7.4 Hz, Ar), 7.65 (t, 1H, *J*=7.2 Hz, Ar), 8.05 (d, 2H, *J*=8.0 Hz, Ar), 8.11 (d, 2H, *J*=7.6 Hz, Ar). **¹³C NMR** (101 MHz, CDCl₃): δ 0.15, 0.18, 1.3, 14.4, 16.2, 18.0, 18.2, 23.2, 24.9, 28.4, 29.3, 29.47, 29.53, 30.3, 31.8, 33.4, 39.7, 93.0,

121.5, 128.7, 129.0, 129.1, 129.3, 131.3, 132.0, 134.9, 140.3, 146.7, 151.6, 153.5, 182.3, 183.0. **^{19}F NMR** (376 MHz, CDCl$_3$) δ -139.62 (21%, ^{10}B-F, DBMBF$_2$), -139.69 (79%, ^{11}B-F, DBMBF$_2$), -146.38-146.63 (m, BODIPY). **^{29}Si NMR** (79 MHz, CDCl$_3$): δ -20.99, 6.96, 7.56. **IR** (KBr, cm^{-1}): 3451, 2956, 2923, 2853, 1604, 1546, 1509, 1490, 1412, 1371, 1308, 1254, 1228, 1199, 1159, 1072, 1042, 984, 837, 795, 714, 687, 636, 597, 564, 519, 479, 418. **HRMS** (ESI) *m/z* calcd. for C$_{47}$H$_{68}$NaB$_2$F$_4$N$_2$O$_4$Si$_3$ [(M+Na)$^+$]: 929.4518, found 929.4513.

MeO-DBMBF$_2$-BODIPY (5 b). **Yield**: 10 %. **^{1}H NMR** (400 MHz, CDCl$_3$): δ 0.01 (s, 6H, SiCH$_3$),

0.04 (s, 6H, SiCH$_3$), 0.07 (s, 6H, SiCH$_3$), 0.49-0.52 (m, 2H, SiCH$_2$), 0.55-0.59 (m, 2H, SiCH$_2$), 1.25 (m, 12H, CH$_2$), 1.42-1.49 (m, 2H, CH$_2$), 1.54-1.62 (m, 2H, CH$_2$) 1.64-1.72 (m, 2H, CH$_2$), 2.38 (s, 6H, CH$_3$), 2.49 (s, 6H, CH$_3$), 2.71 (t, 2H, *J*=7.6 Hz, CH$_2$), 2.88 (m, 2H, CH$_2$), 3.90 (s, 3H, OCH$_3$), 6.01 (s, 2H, BODIPY-CH), 6.99 (d, 2H, *J*=9.0 Hz, Ar), 7.05 (s, 1H, COCHCO), 7.31 (d, 2H, *J*=8.3 Hz, Ar), 8.02 (d, 2H, *J*=8.3 Hz, Ar), 8.11 (d, 2H, *J*=9.0 Hz, Ar). **^{13}C NMR** (101 MHz, CDCl$_3$): δ 0.17, 0.21, 1.3, 14.4, 16.3, 18.0, 18.2, 23.2, 25.0, 28.4, 29.3, 29.4, 29.5, 29.6, 30.4, 31.8, 33.4, 39.7, 55.7, 92.1, 114.6, 121.5, 124.23, 128.8, 129.2, 129.7, 131.38, 131.42, 140.3, 146.7, 150.9, 153.6, 165.5, 181.4, 181.6. **^{19}F NMR** (376 MHz, CDCl$_3$) δ -140.41 (21%, ^{10}B-F, DBMBF$_2$), -140.47 (79%, ^{11}B-F, DBMBF$_2$), -146.38-146.63 (m, BODIPY). **^{29}Si NMR** (79 MHz, CDCl$_3$): δ -21.03, 6.96, 7.53. **IR** (KBr, cm^{-1}): 2956, 2924, 2854, 1639, 1608, 1549, 1500, 1466, 1413, 1373, 1311, 1252, 1200, 1177, 1162, 1043, 986, 842, 796, 712, 630, 613, 594, 553, 520, 478. **HRMS** (ESI) *m/z* calcd. for C$_{48}$H$_{70}$NaB$_2$F$_4$N$_2$O$_5$Si$_3$ [(M+Na)$^+$]: 959.4624, found 959.4621.

1-(PropylDBMBF$_2$)-1,1,3,3,3-pentamethyldisiloxane (6 a). It was synthesized by the method described earlier by us.[6]
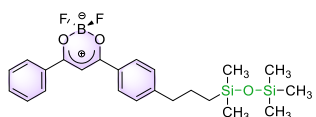
1-(PropylDBMBF$_2$-OCH$_3$)-1,1,3,3,3-pentamethyldisiloxane (6 b). It was synthesized by the method described earlier by us.[6]
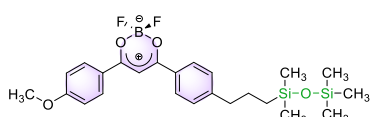
3. Spectral Data
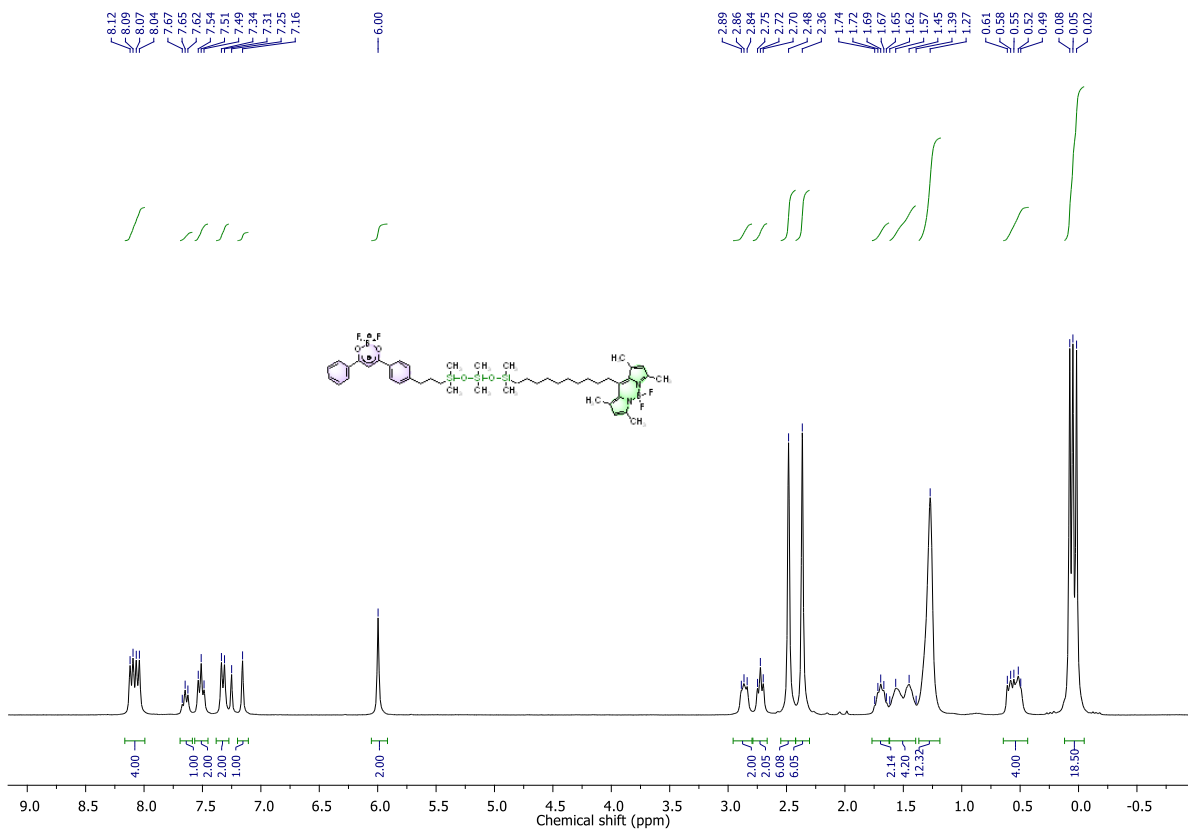
Figure S1. ^{1}H NMR spectrum of **5 a** in CDCl$_3$.
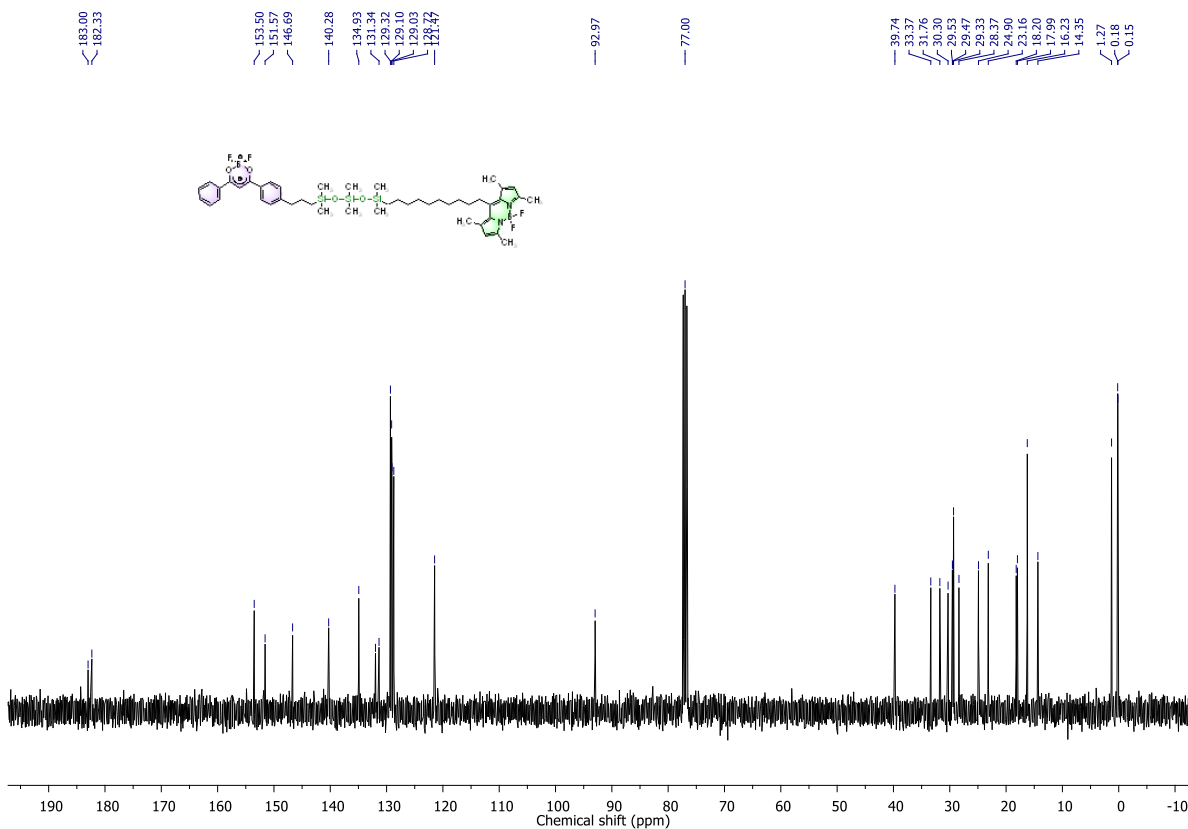
Figure S2. ^{13}C NMR spectrum of **5 a** in CDCl$_3$.
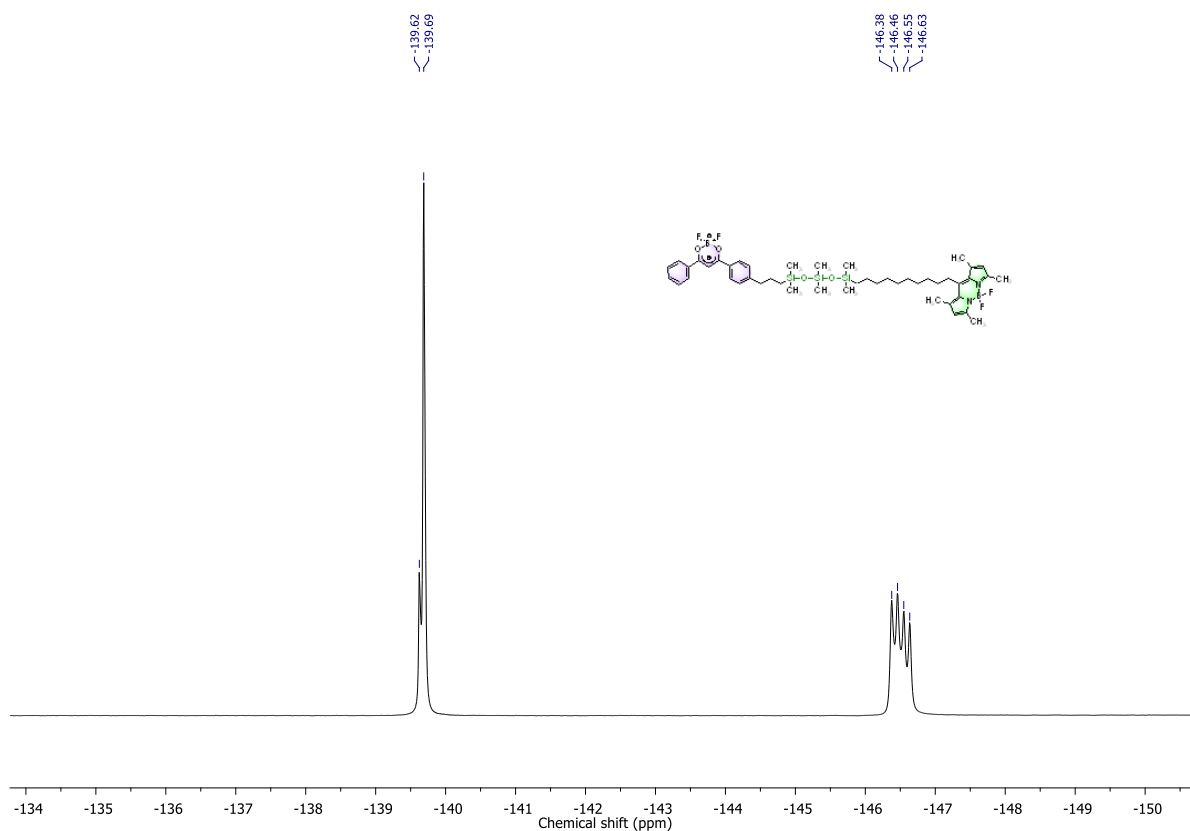
Figure S3. ^{19}F NMR spectrum of **5 a** in CDCl$_3$.
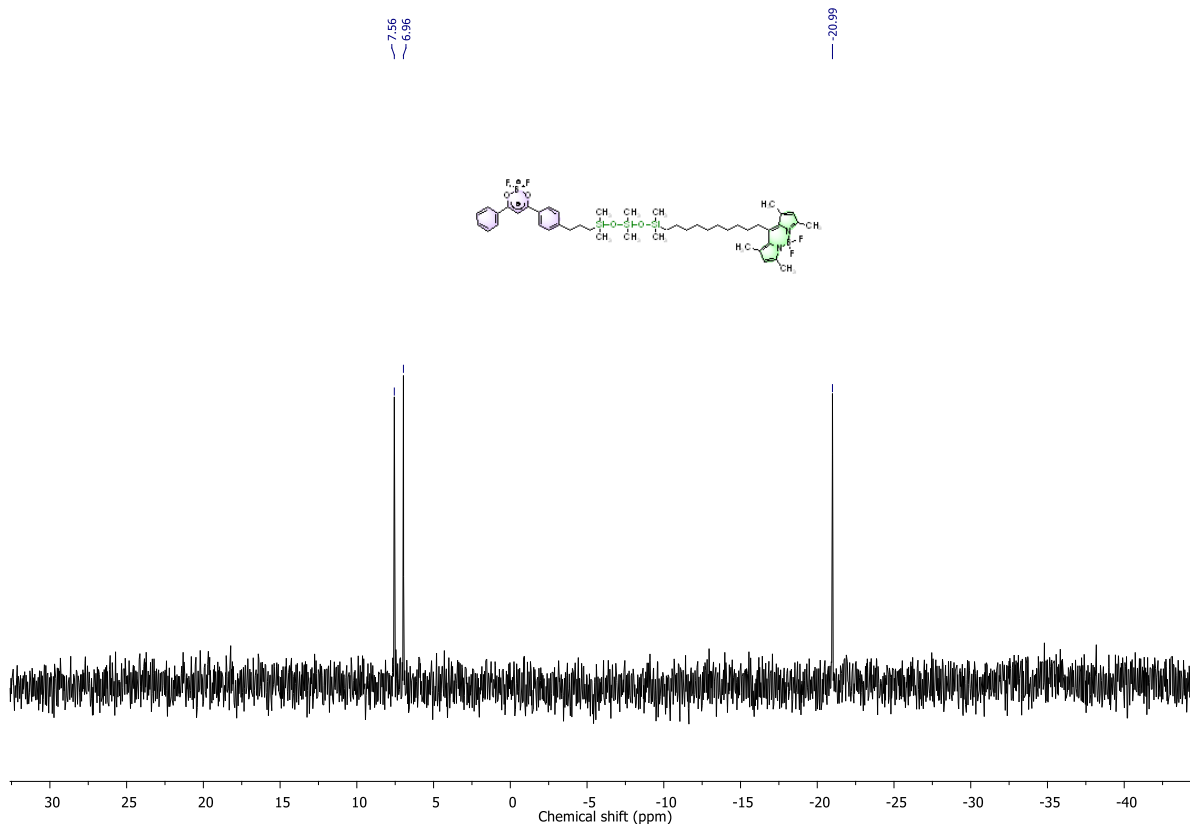
Figure S4. ^{29}Si NMR spectrum of **5 a** in CDCl$_3$.
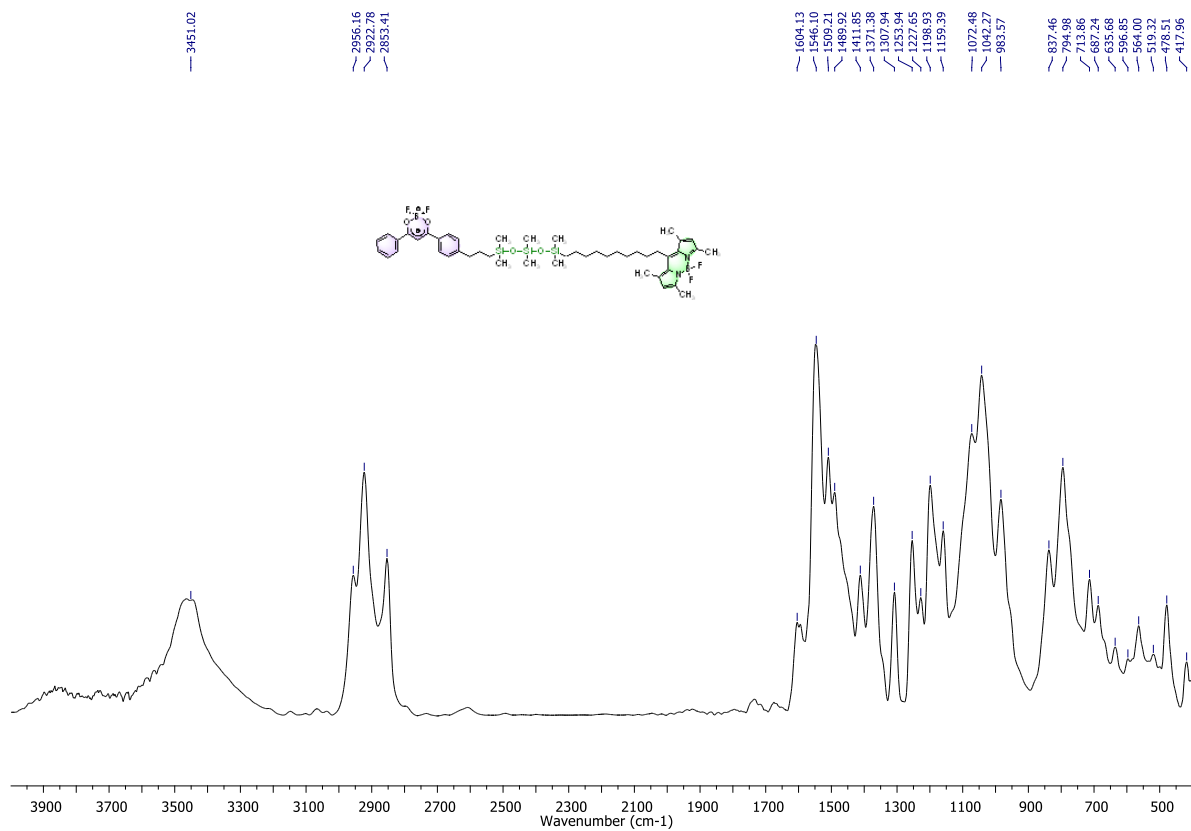
Figure S5. IR spectrum of **5 a**.
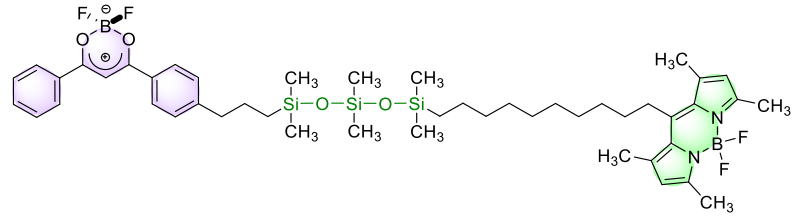
m/z calcd. for $C_{47}H_{68}NaB_2F_4N_2O_4Si_3$ [(M+H)$^+$]: 929.4518
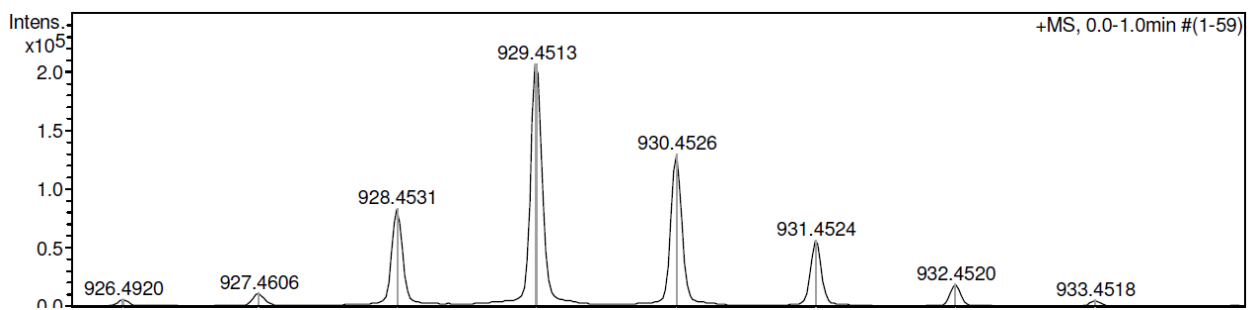
Figure S6. Mass-spectrum of **5 a**.
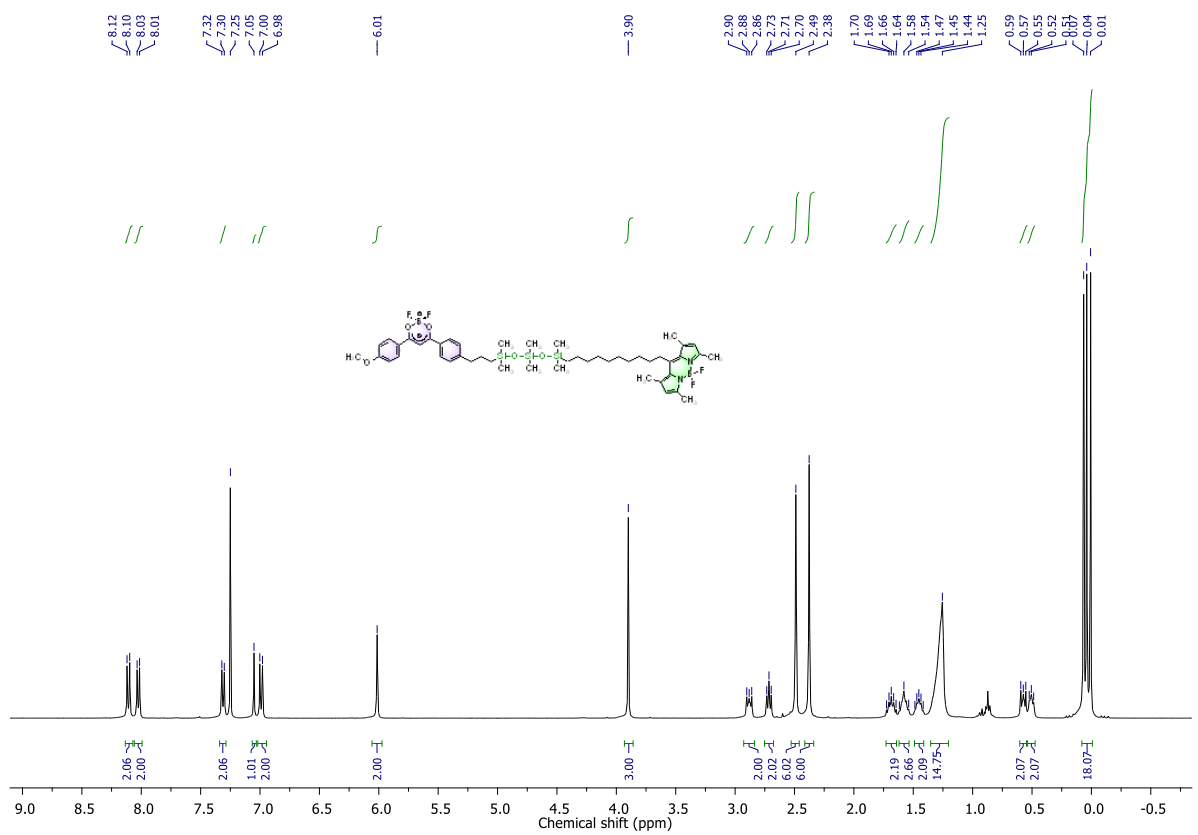
Figure S7. ^{1}H NMR spectrum of **5 b** in CDCl$_3$.
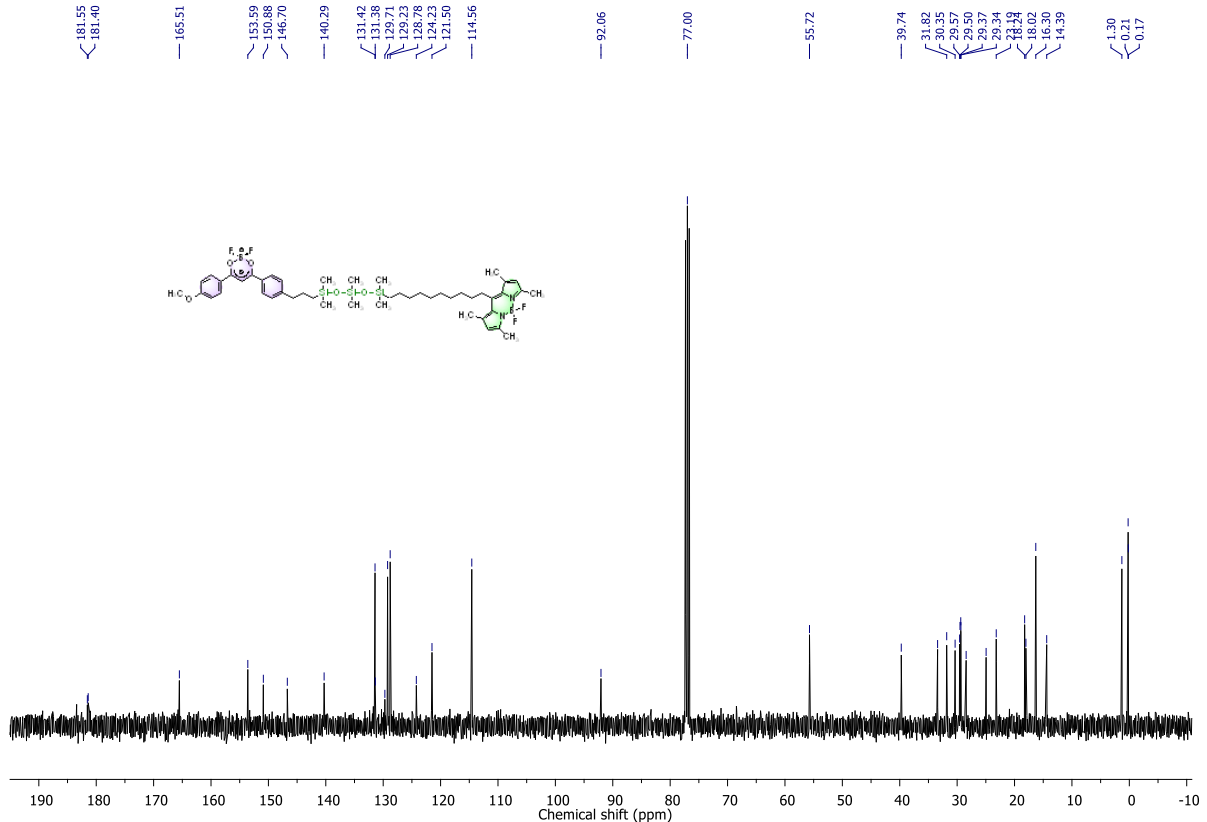
Figure S8. ^{13}C NMR spectrum of **5 b** in CDCl$_3$.
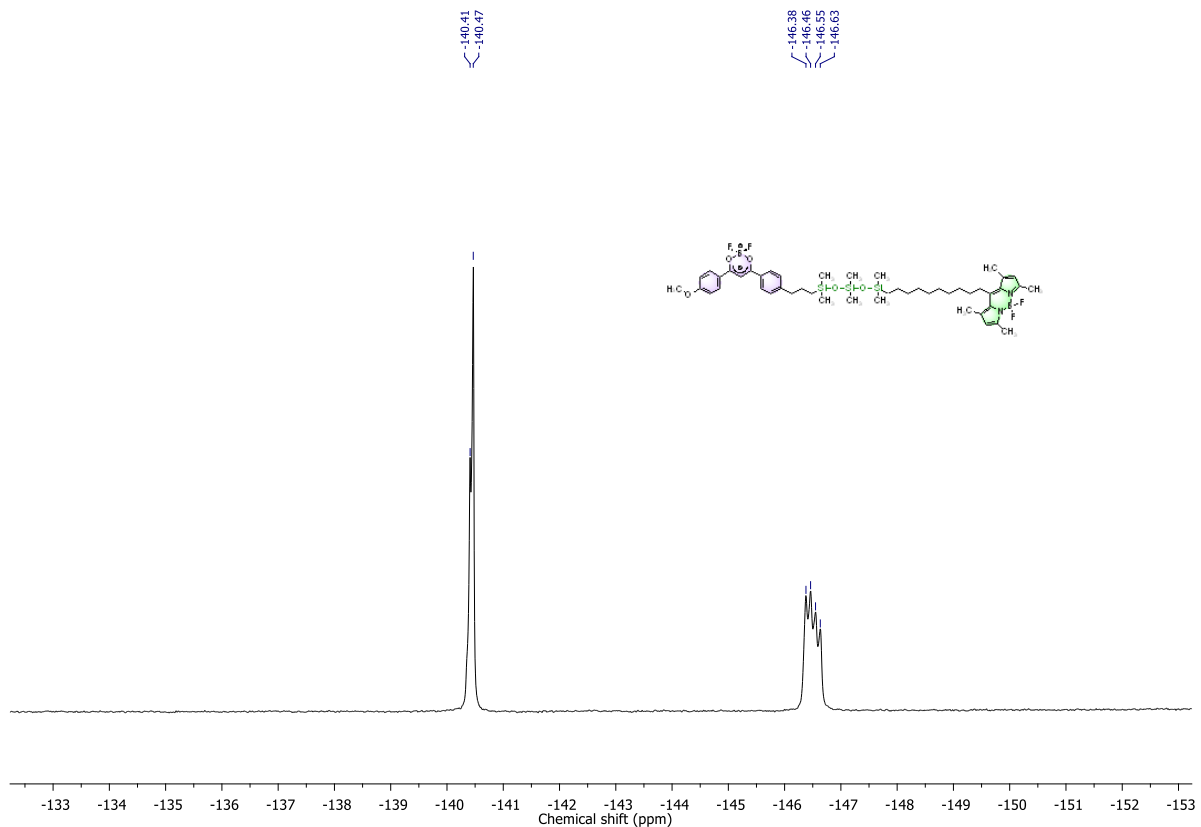
Figure S9. ^{19}F NMR spectrum of **5 b** in CDCl$_3$.
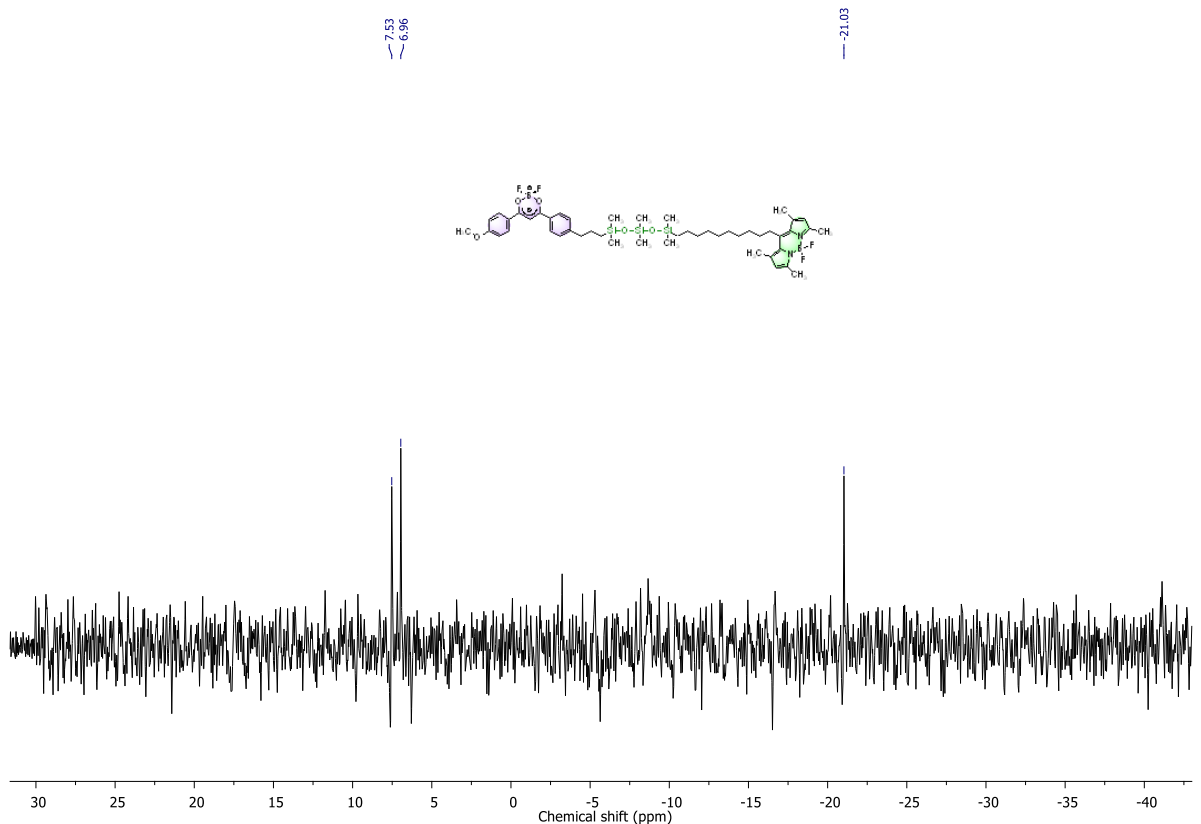
Figure S10. ^{29}Si NMR spectrum of **5 b** in CDCl$_3$.
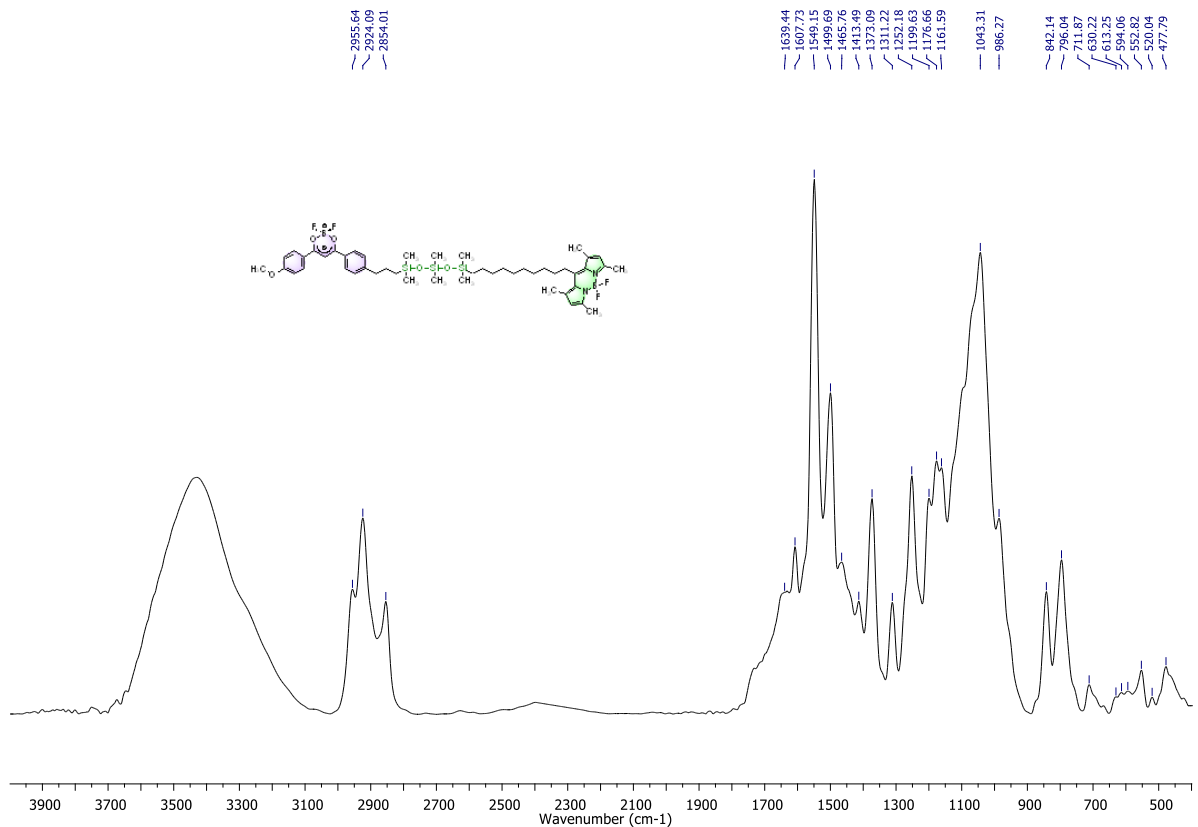
Figure S11. IR spectrum of **5 b**.
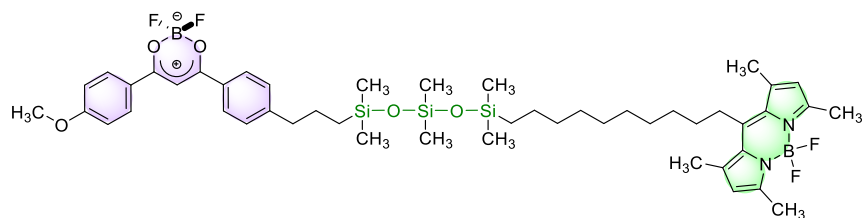
m/z calcd. for $C_{48}H_{70}NaB_2F_4N_2O_5Si_3$ [(M+H)$^+$]: 959.4624
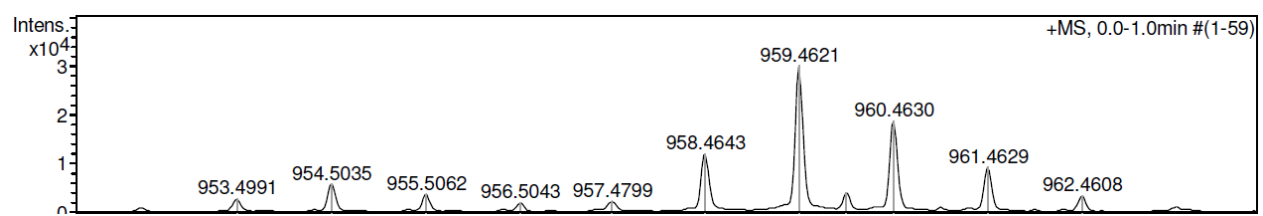
Figure S12. Mass-spectrum of **5 b**.

4. Absorption and Emission Spectra
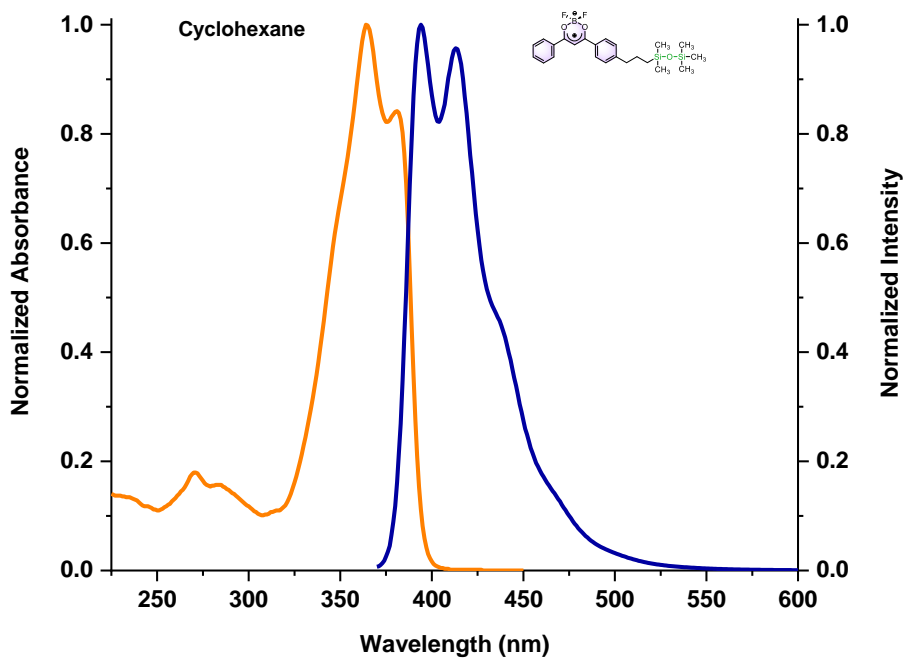
Figure S13. Normalized UV-visible absorption and emission spectra of **6 a** in cyclohexane (c = 1×10^{-6} M) at room temperature.
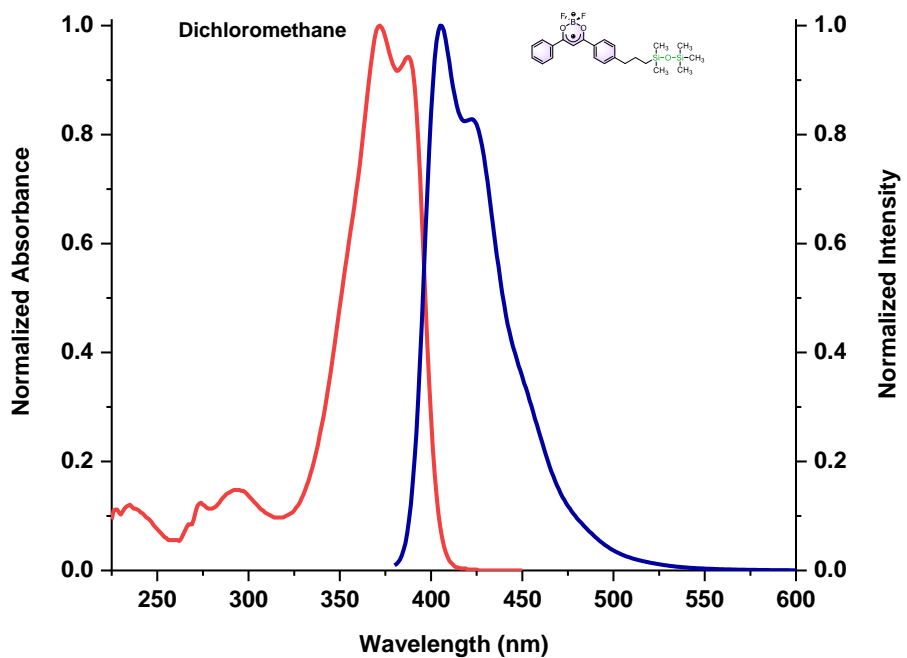

Figure S14. Normalized UV-visible absorption and emission spectra of **6 a** in dichloromethane (c = 1×10^{-6} M) at room temperature.[4]
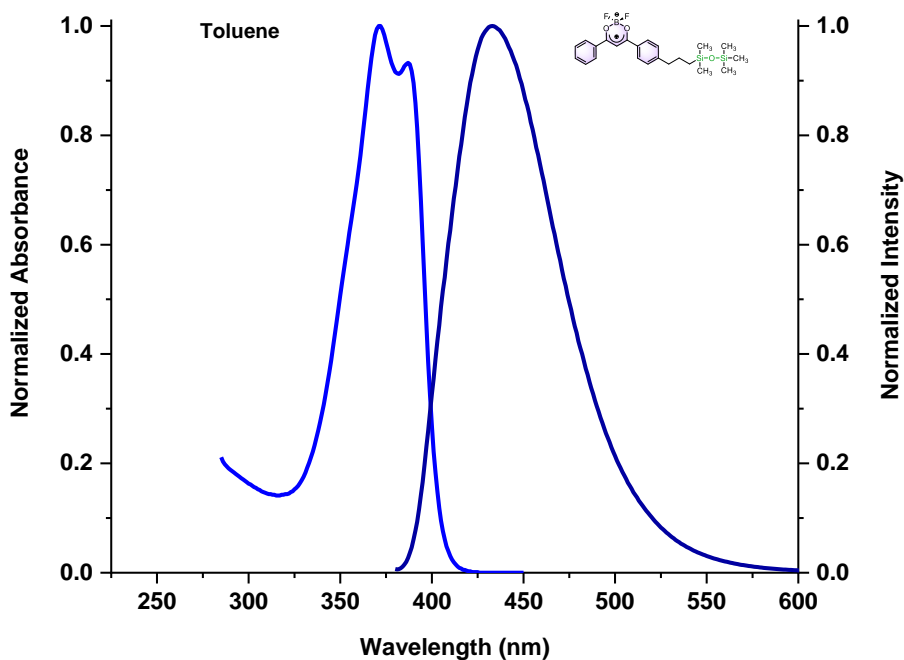
Figure S15. Normalized UV-visible absorption and emission spectra of **6 a** in toluene (c = 1 × 10⁻⁶ M) at room temperature.
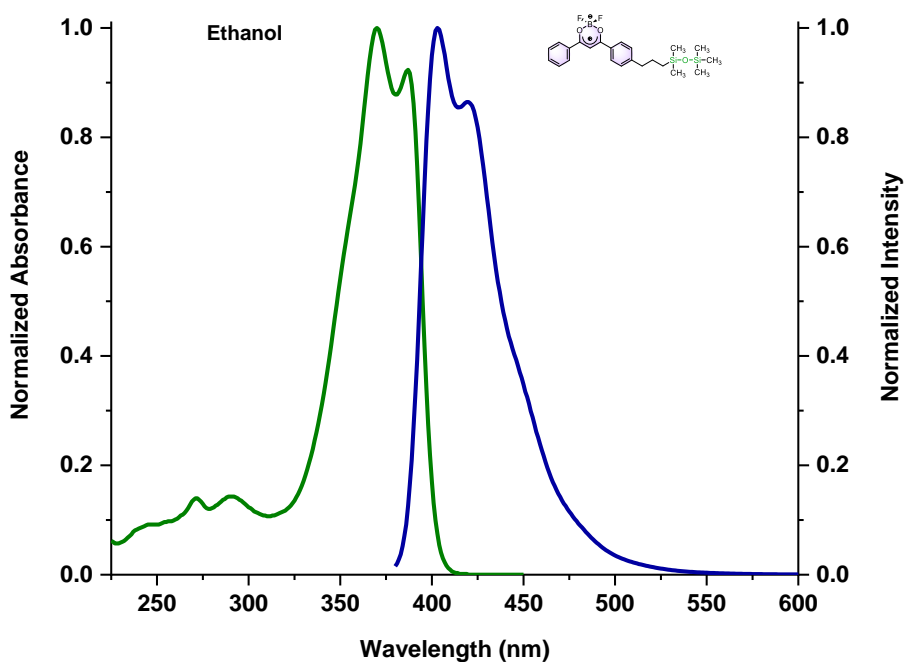

Figure S16. Normalized UV-visible absorption and emission spectra of **6 a** in ethanol (c = 1 × 10⁻⁶ M) at room temperature.
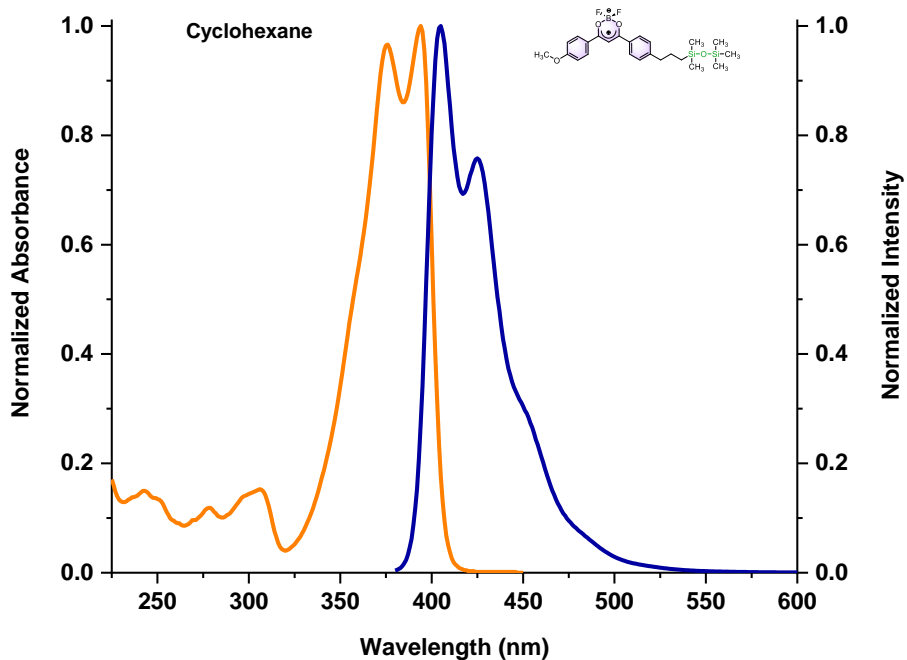
Figure S17. Normalized UV-visible absorption and emission spectra of **6 b** in cyclohexane (c = 1 × 10⁻⁶ M) at room temperature.
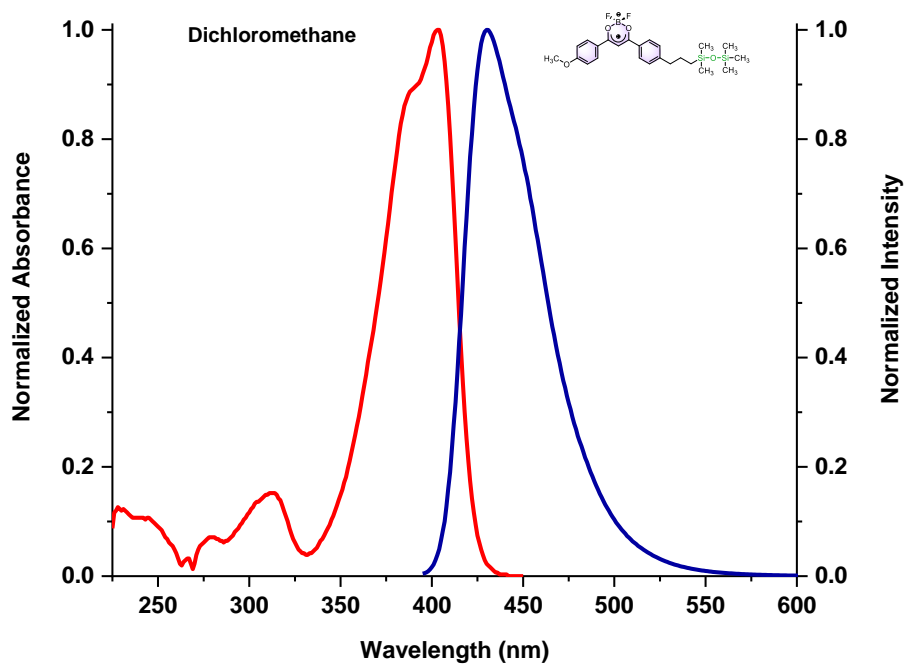
Figure S18. Normalized UV-visible absorption and emission spectra of **6 b** in dichloromethane (c = 1 × 10⁻⁶ M) at room temperature.
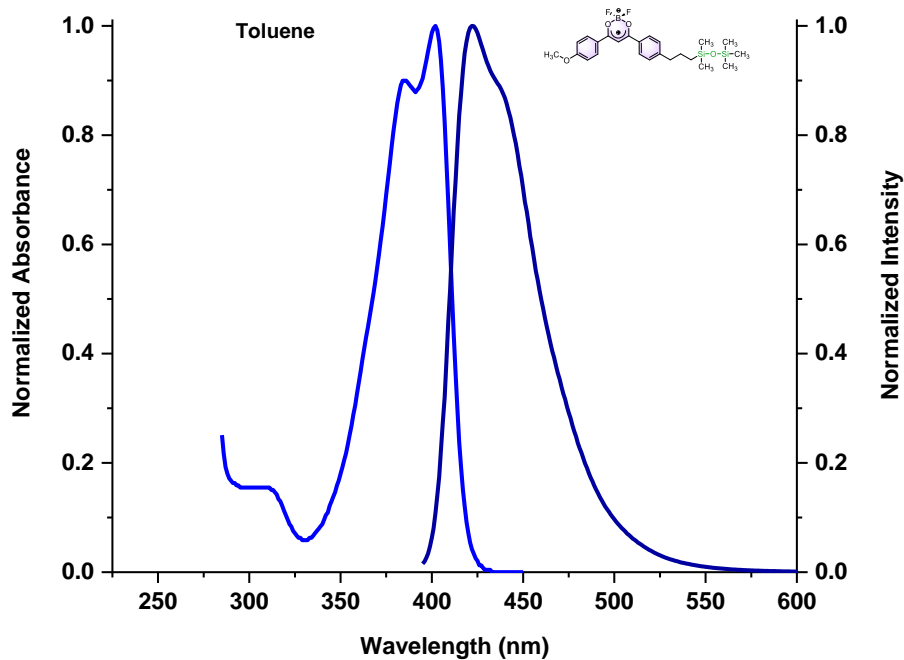
Figure S19. Normalized UV-visible absorption and emission spectra of **6 b** in toluene (c = 1 × 10⁻⁶ M) at room temperature.
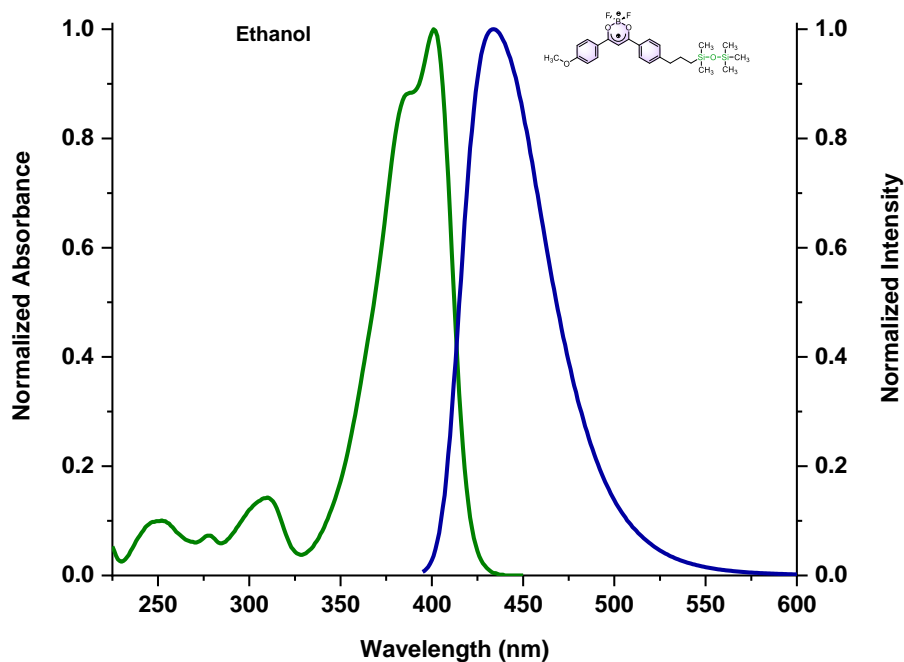
Figure S20. Normalized UV-visible absorption and emission spectra of **6 b** in ethanol (c = 1 × 10⁻⁶ M) at room temperature.
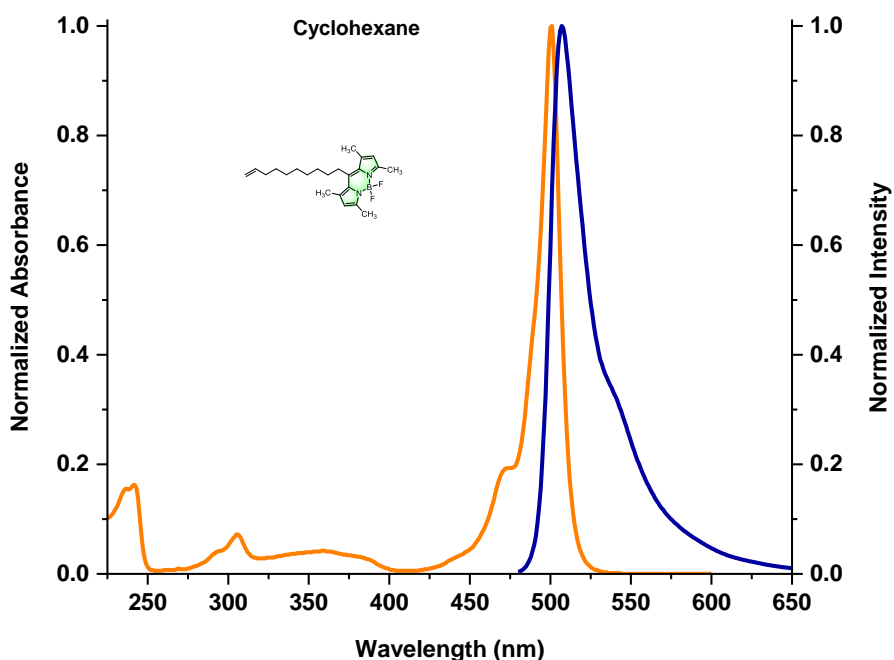
Figure S21. Normalized UV-visible absorption and emission spectra of **4** in cyclohexane (c = 1 × 10⁻⁶ M) at room temperature.
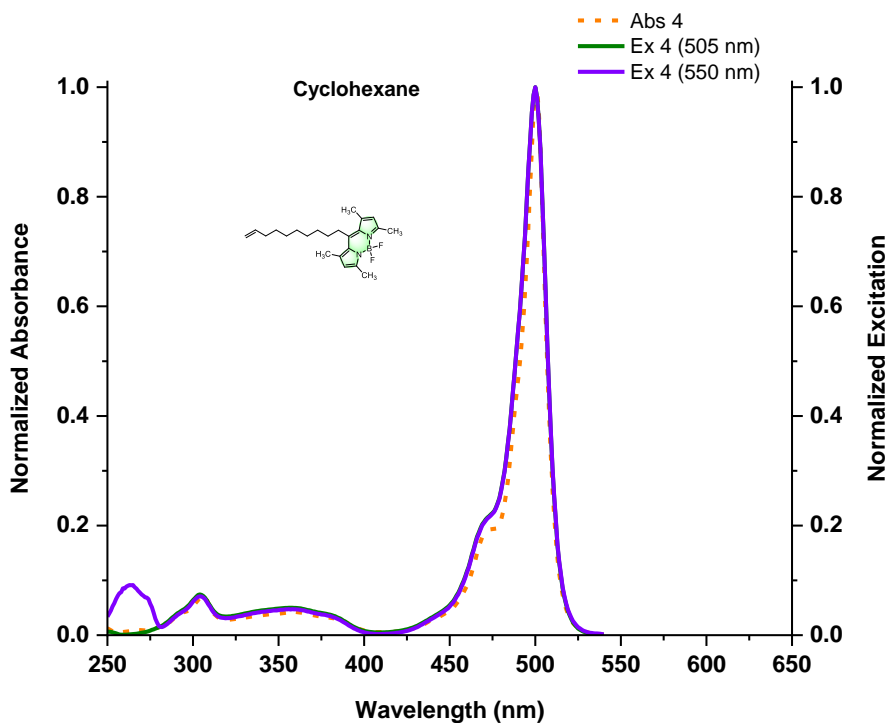
**Figure S22.** Normalized UV-visible absorption and excitation spectra of **4** in cyclohexane (c = 1 × 10⁻⁶ M) at room temperature.
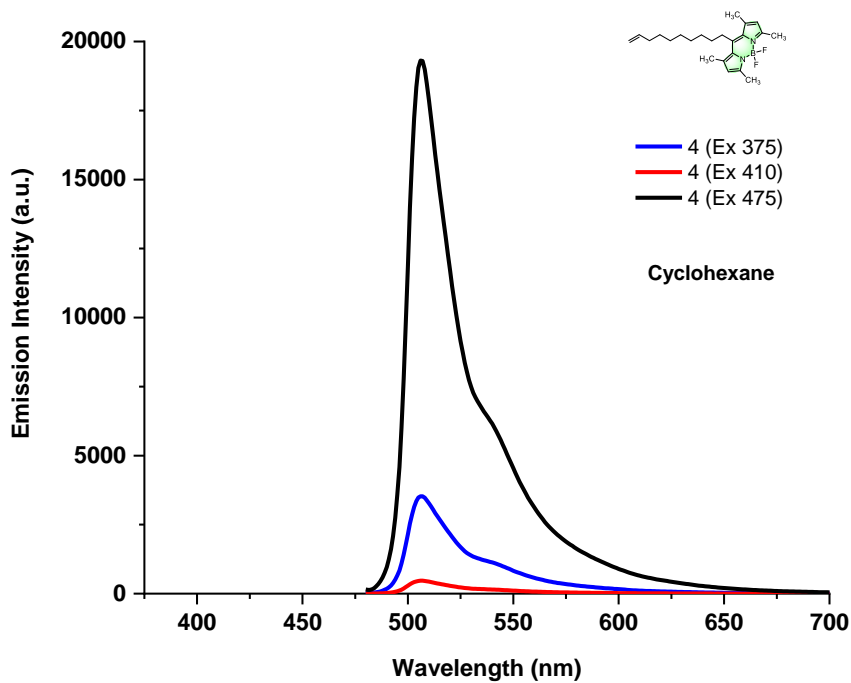
Figure S23. Emission spectra of **4** in cyclohexane at different excitation wavelengths (375, 410 and 475 nm) at room temperature.
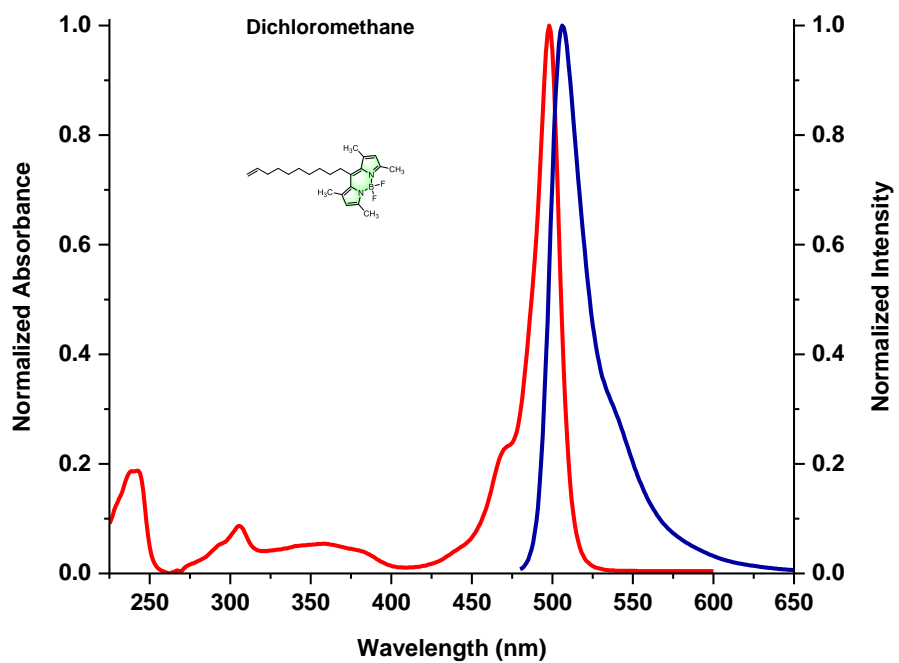
Figure S24. Normalized UV-visible absorption and emission spectra of **4** in dichloromethane (c = 1 × 10⁻⁶ M) at room temperature.
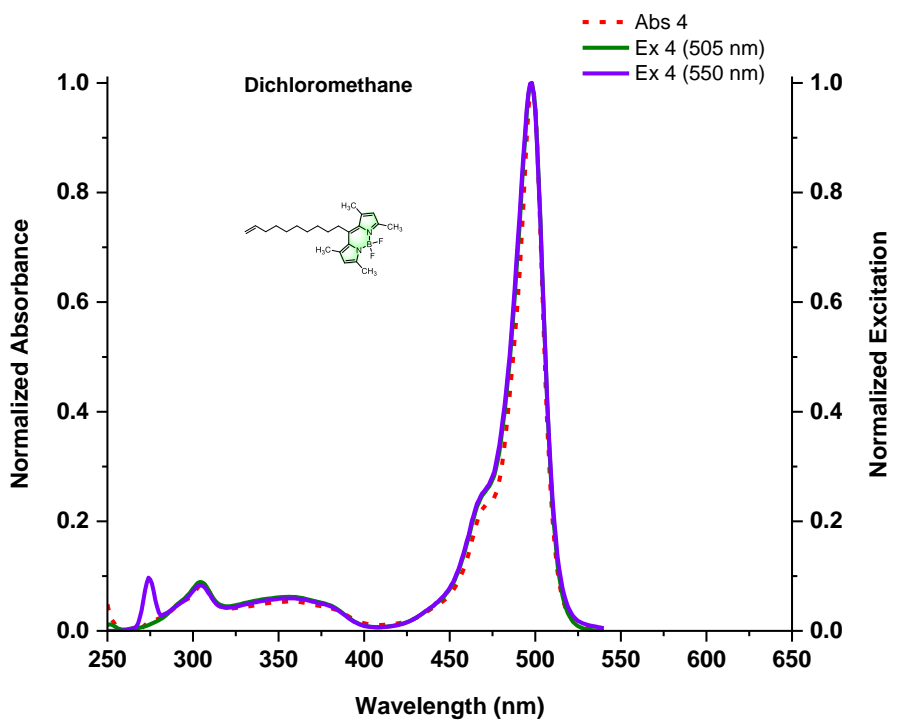
Figure S25. Normalized UV-visible absorption and excitation spectra of **4** in dichloromethane (c = 1 × 10⁻⁶ M) at room temperature.
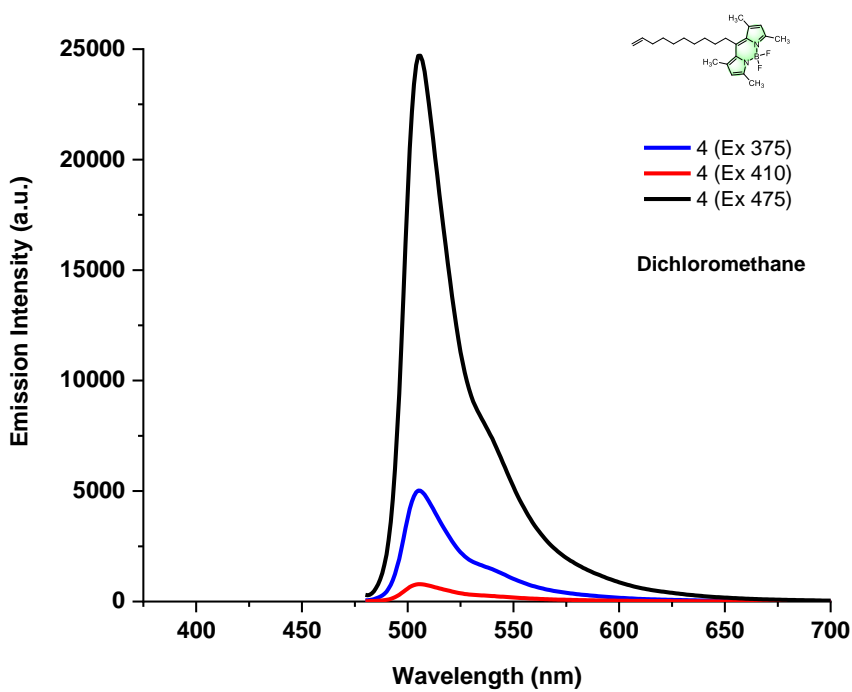

Figure S26. Emission spectra of **4** in dichloromethane (c = 1 × 10⁻⁶ M) at different excitation wavelengths (375, 410 and 475 nm) at room temperature.
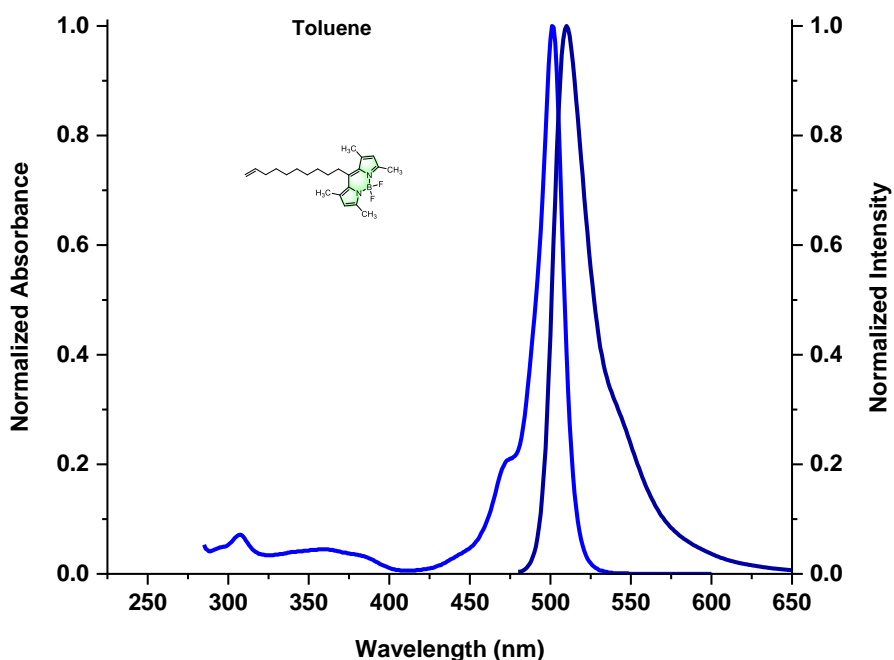
Figure S27. Normalized UV-visible absorption and emission spectra of **4** in toluene (c = 1 × 10⁻⁶ M) at room temperature.
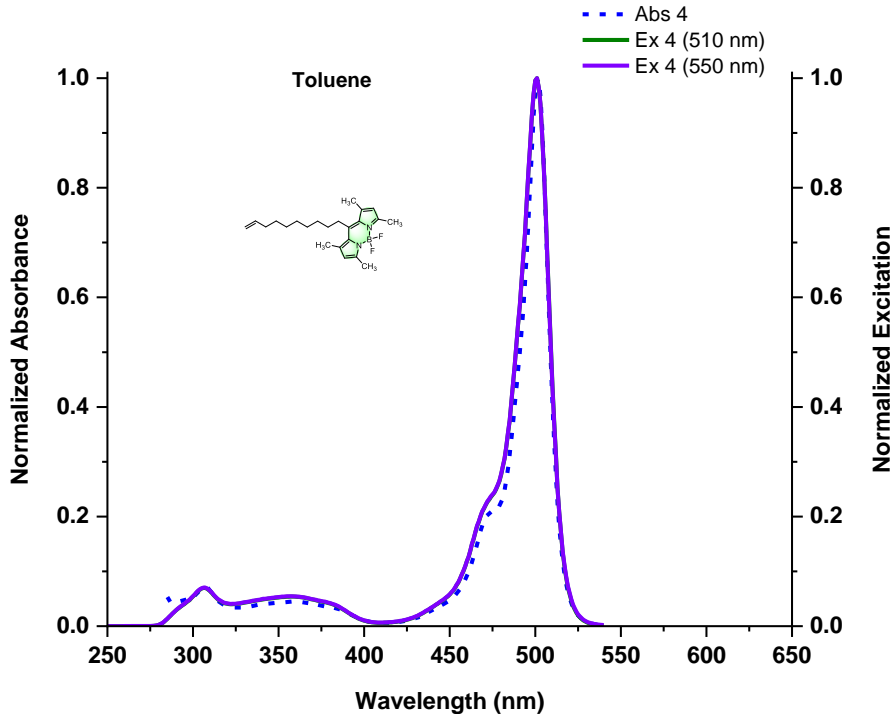
Figure S28. Normalized UV-visible absorption and excitation spectra of **4** in toluene (c = 1 × 10⁻⁶ M) at room temperature.
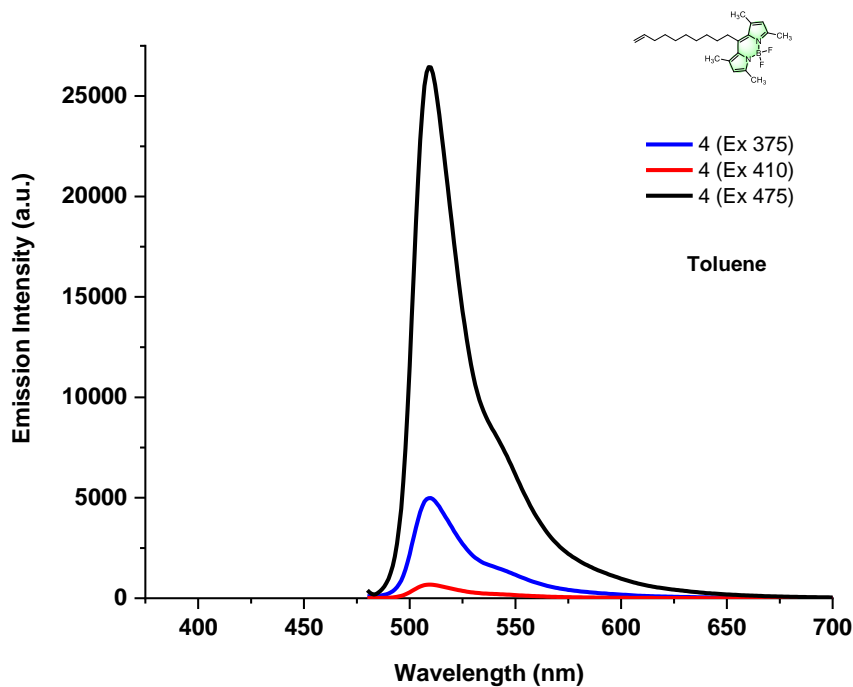
Figure S29. Emission spectra of **4** in toluene (c = 1 × 10^{-6} M) at different excitation wavelengths (375, 410 and 475 nm) at room temperature.
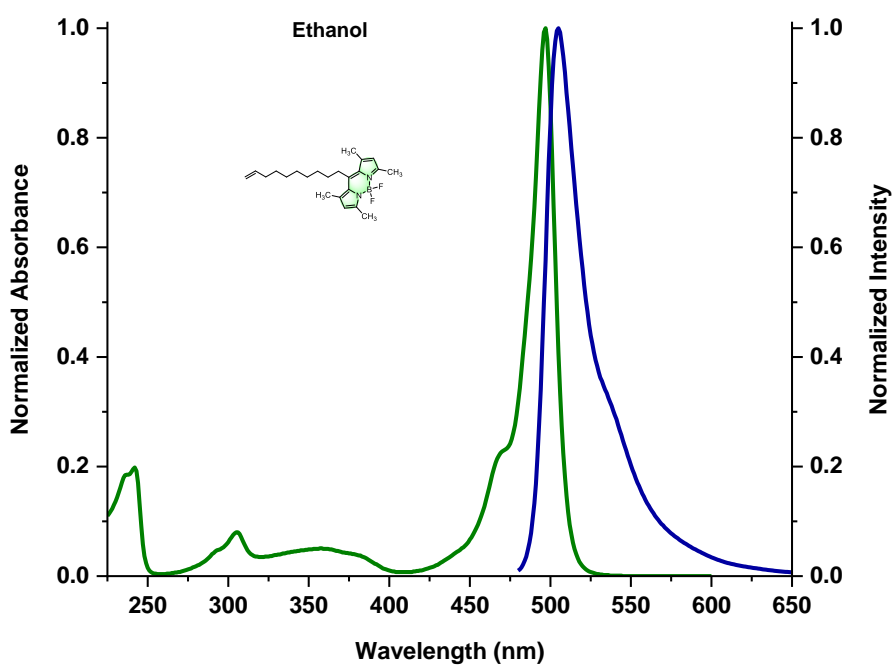

Figure S30. Normalized UV-visible absorption and emission spectra of **4** in ethanol (c = 1 × 10^{-6} M) at room temperature.
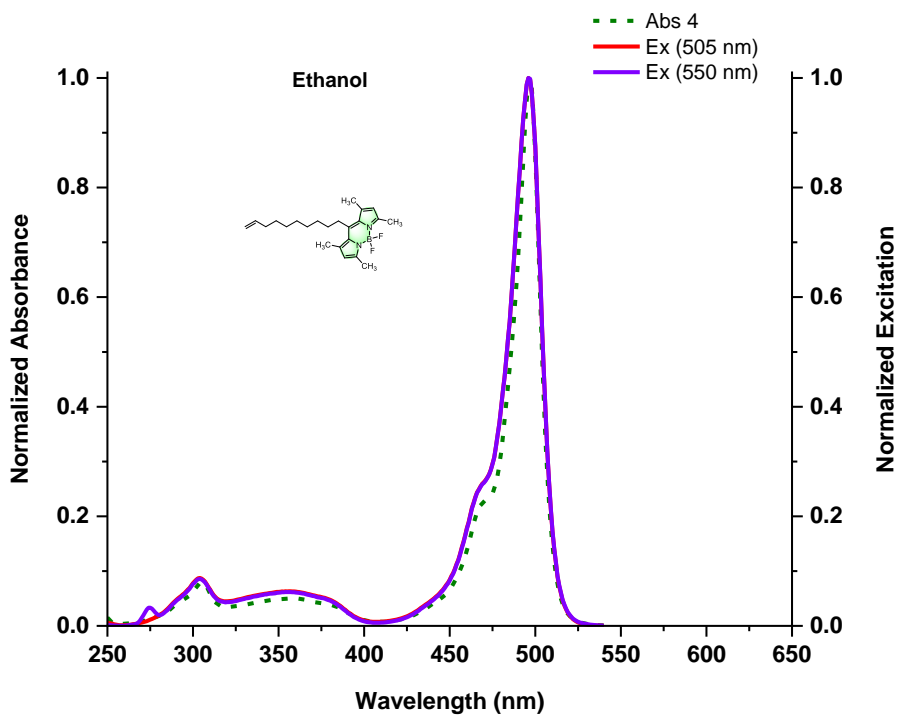
Figure S31. Normalized UV-visible absorption and excitation spectra of **4** in ethanol (c = 1 × 10^{-6} M) at room temperature.
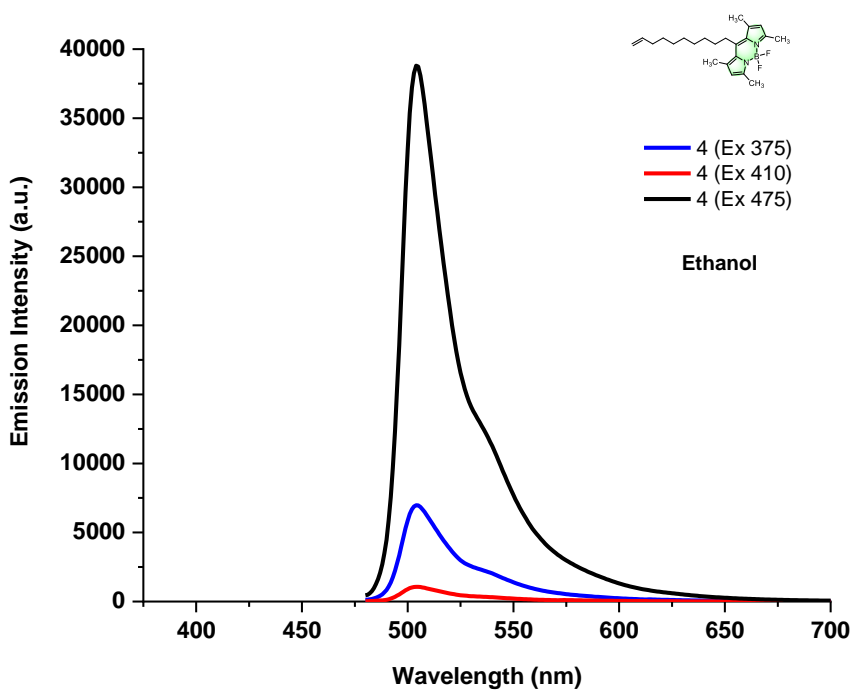
**Figure S32.** Emission spectra of **4** in ethanol (c = 1 × 10^{-6} M) at different excitation wavelengths (375, 410 and 475 nm) at room temperature.
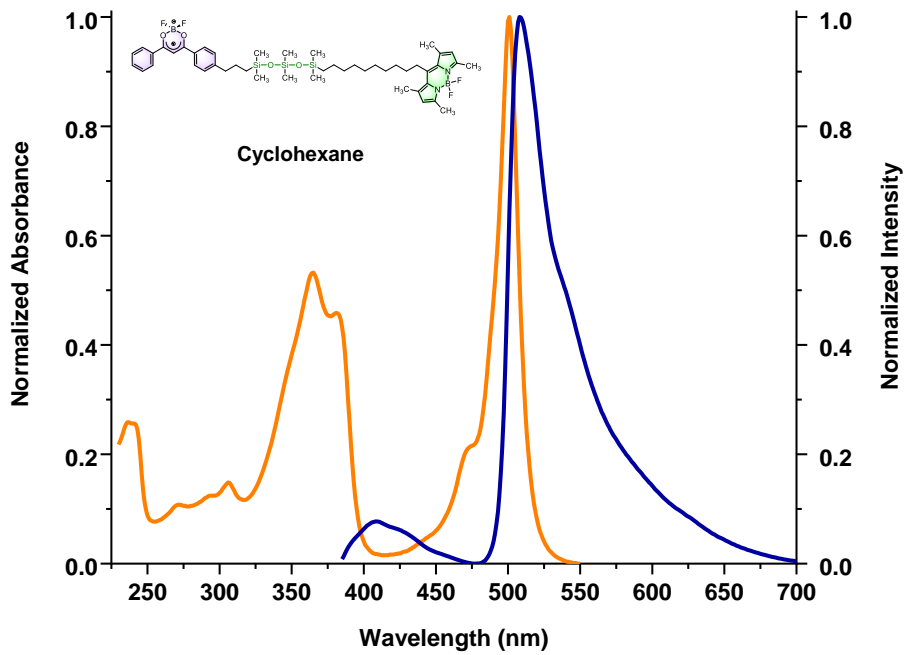
Figure S33. Normalized UV-visible absorption and emission spectra of **5 a** in cyclohexane (c = 1×10^{-6} M) at room temperature. Excitation at 375 nm.
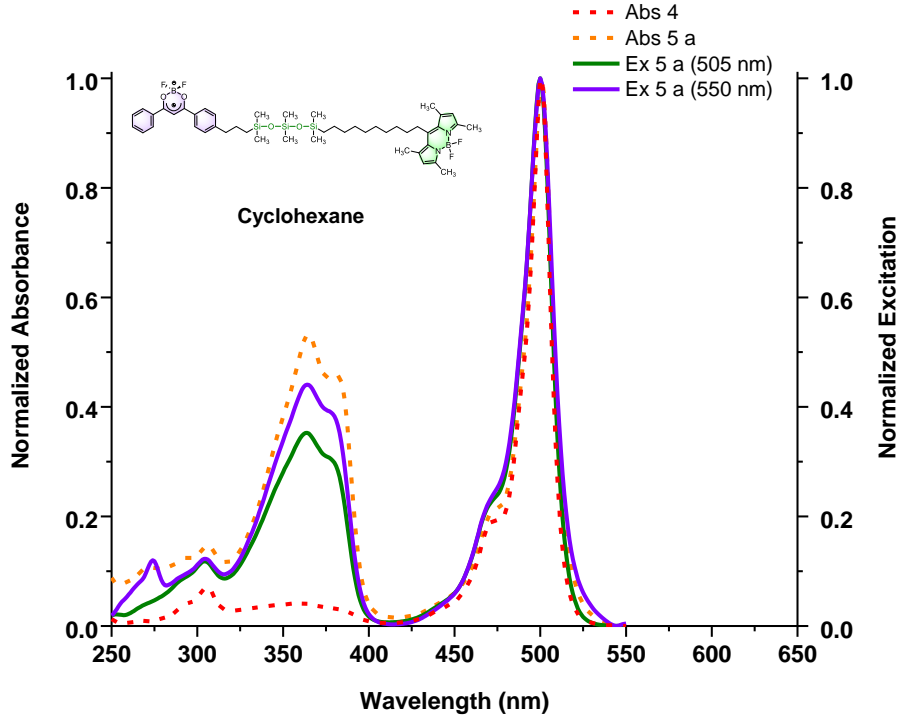

Figure S34. Normalized UV-visible absorption and excitation spectra of **5 a** in cyclohexane (c = 1×10^{-6} M) at room temperature.
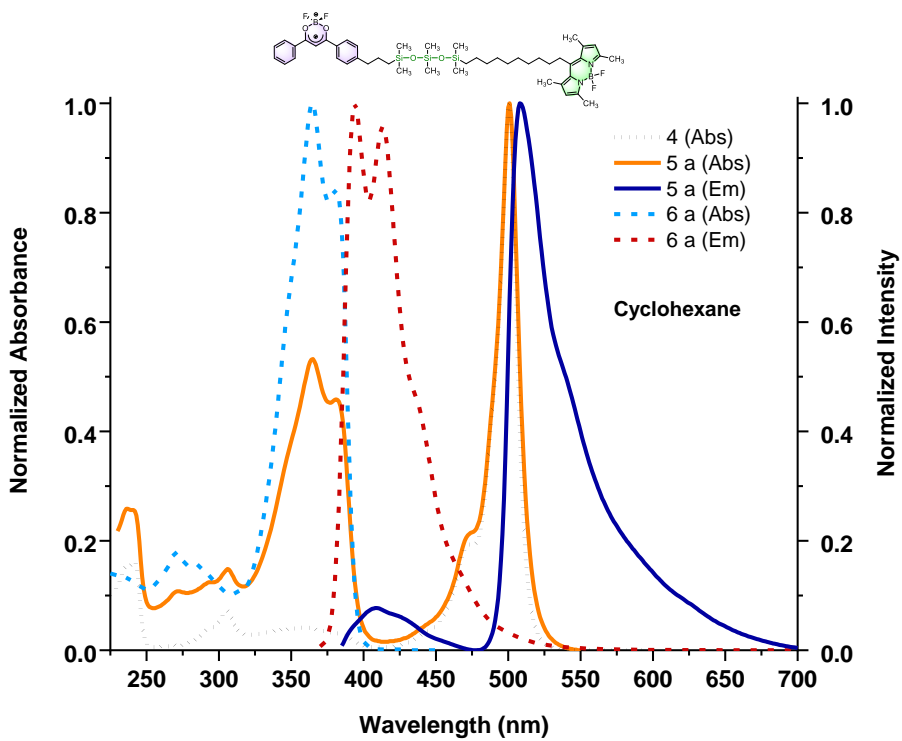
Figure S35. Normalized UV-visible absorption and emission spectra of **4**, **5 a** and **6 a** in cyclohexane (c = 1 × 10^{-6} M) at room temperature.
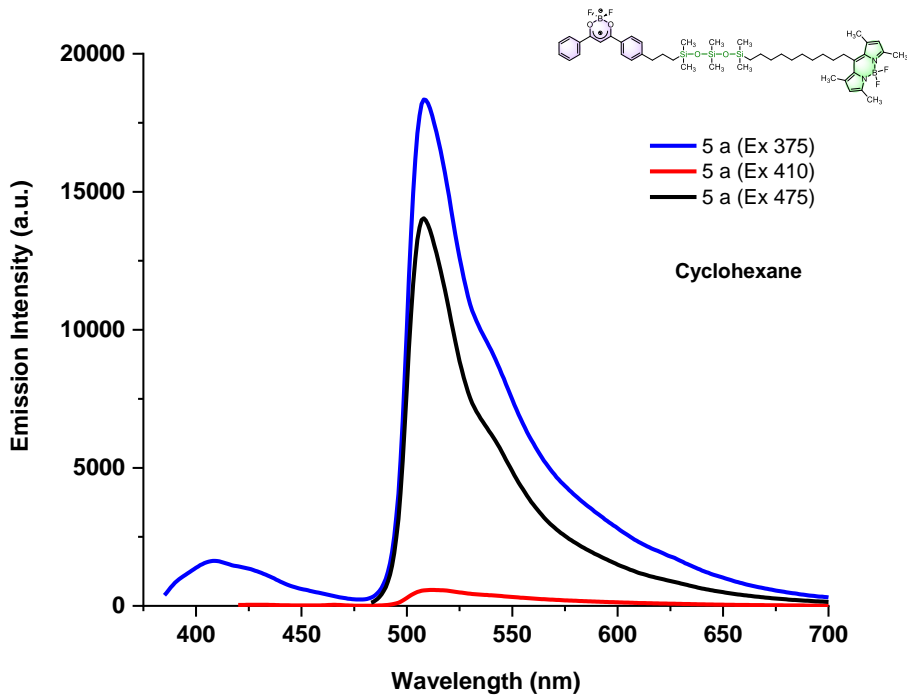

Figure S36. Emission spectra of **5 a** in cyclohexane at different excitation wavelengths (375, 410 and 475 nm) at room temperature.
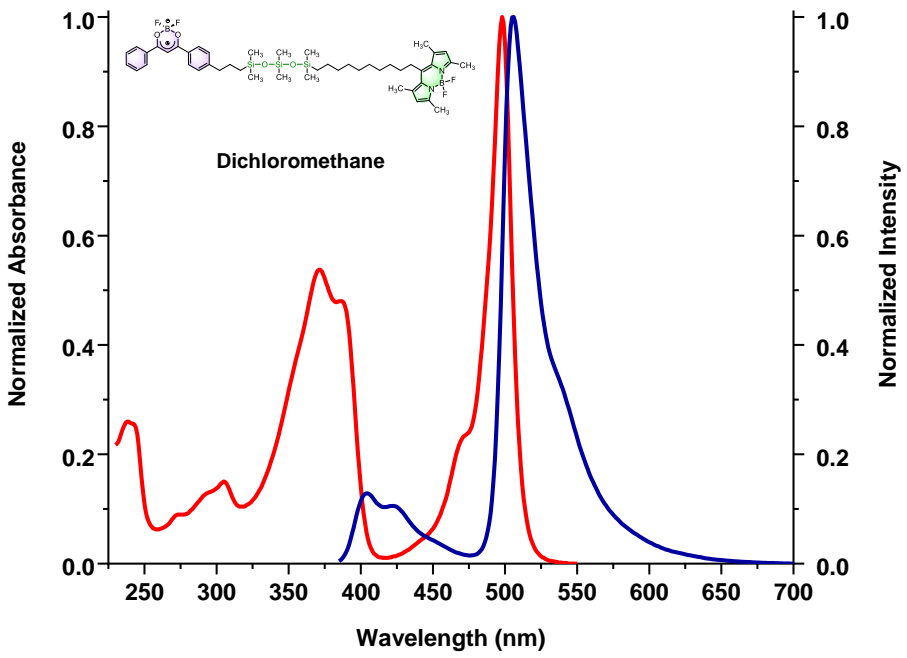
Figure S37. Normalized UV-visible absorption and emission spectra of **5 a** in dichloromethane (c = 1 × 10⁻⁶ M) at room temperature. Excitation at 375 nm.
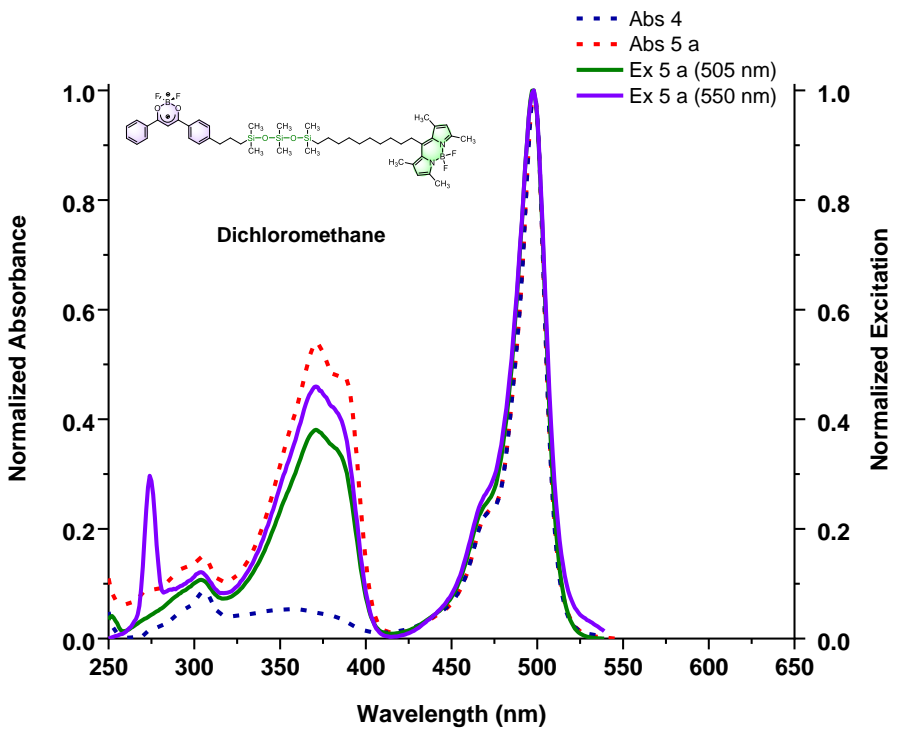
Figure S38 Normalized UV-visible absorption and excitation spectra of **5 a** in dichloromethane (c = 1 × 10⁻⁶ M) at room temperature.
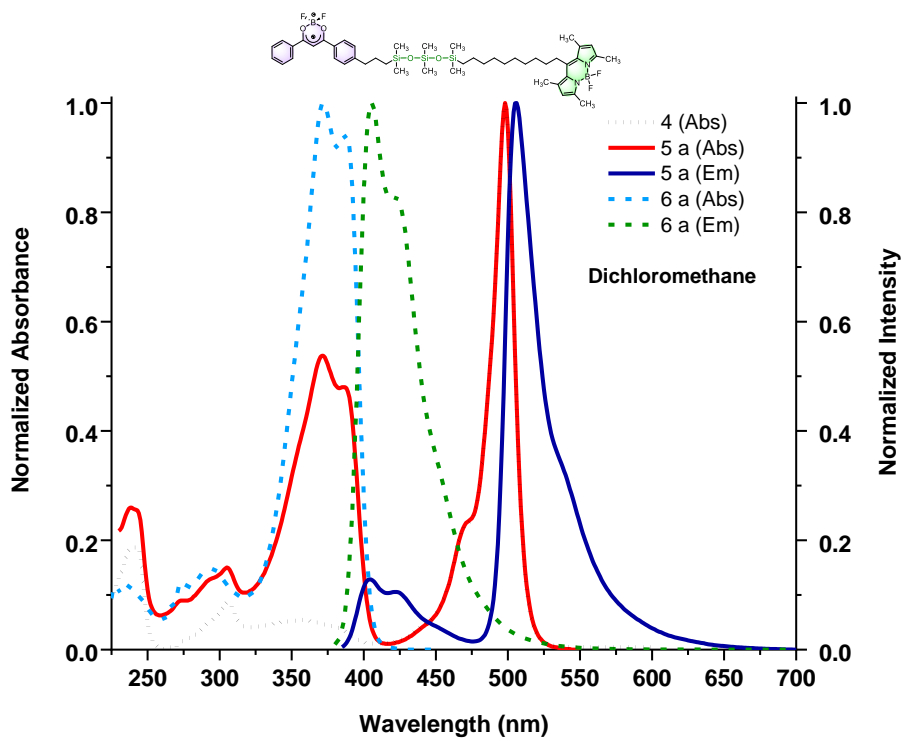
Figure S39. Normalized UV-visible absorption and emission spectra of **4**, **5 a** and **6 a** in dichloromethane (c = 1 × 10⁻⁶ M) at room temperature.
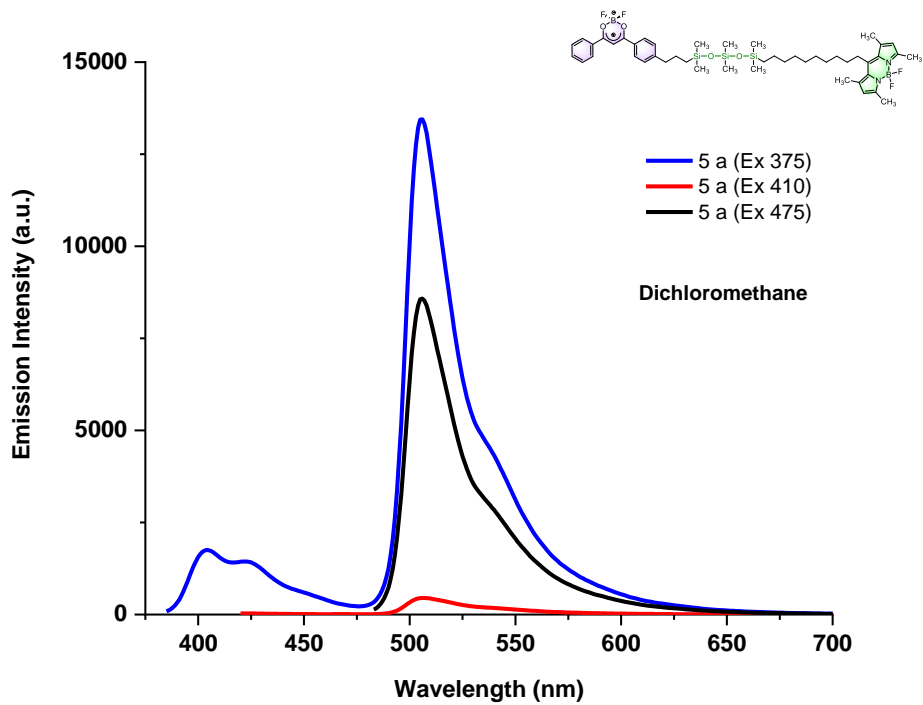
Figure S40. Emission spectra of **5 a** in dichloromethane (c = 1 × 10⁻⁶ M) at different excitation wavelengths (375, 410 and 475 nm) at room temperature.
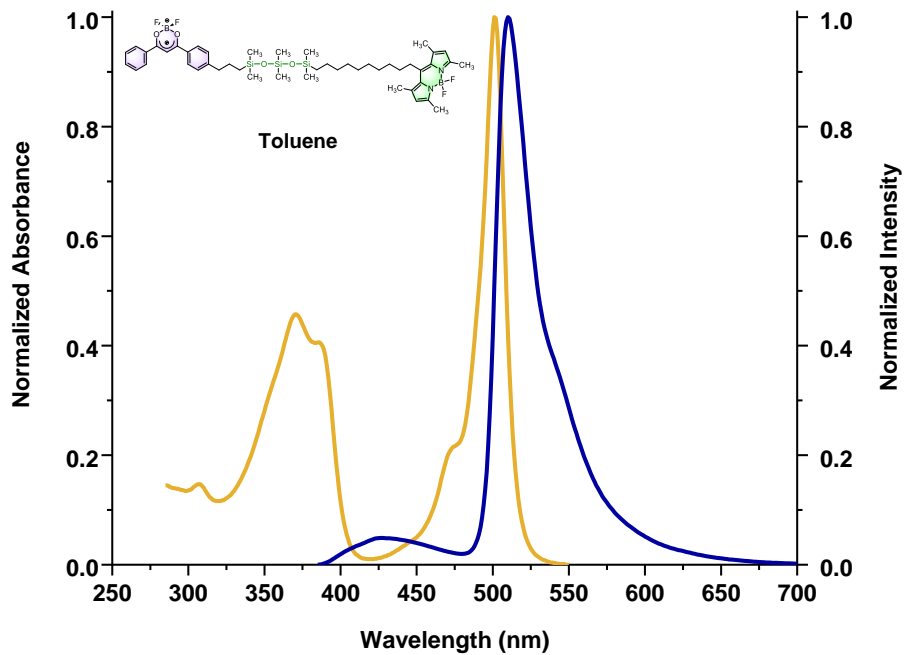
Figure S41. Normalized UV-visible absorption and emission spectra of **5 a** in toluene (c = 1 ×
10^{-6} M) at room temperature. Excitation at 375 nm.
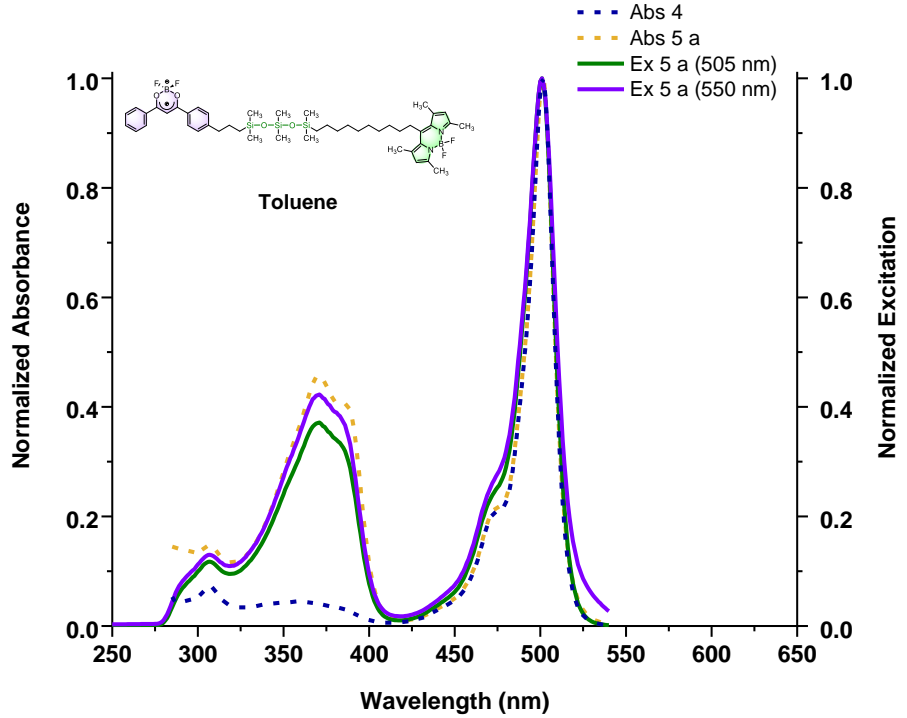
Figure S42. Normalized UV-visible absorption and excitation spectra of **5 a** in toluene (c = 1 ×
10^{-6} M) at room temperature.
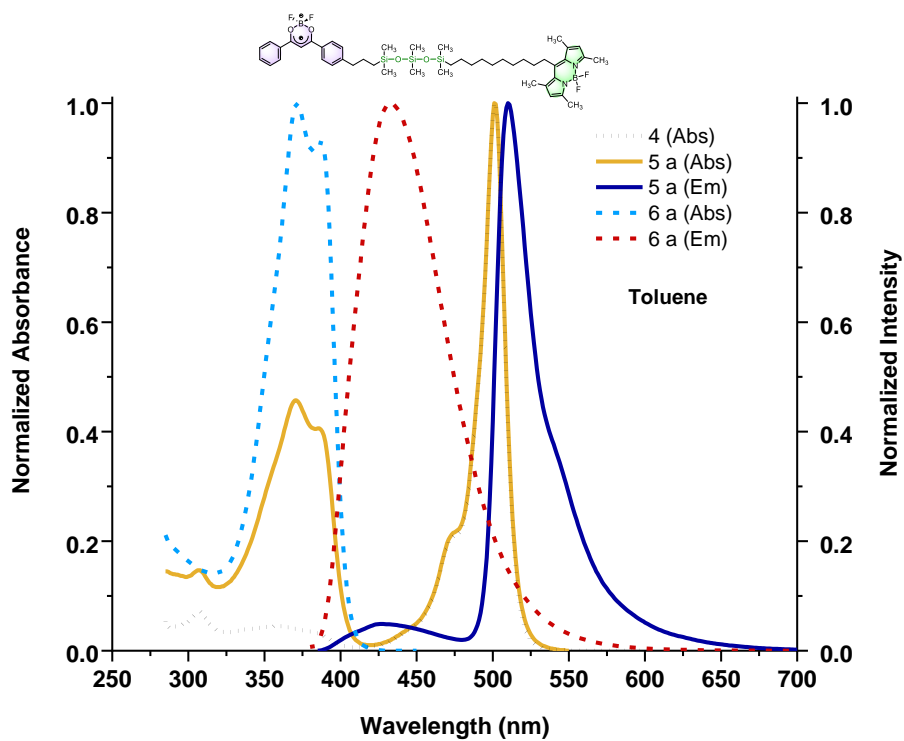
Figure S43. Normalized UV-visible absorption and emission spectra of **4**, **5 a** and **6 a** in toluene (c = 1 × 10^{-6} M) at room temperature.
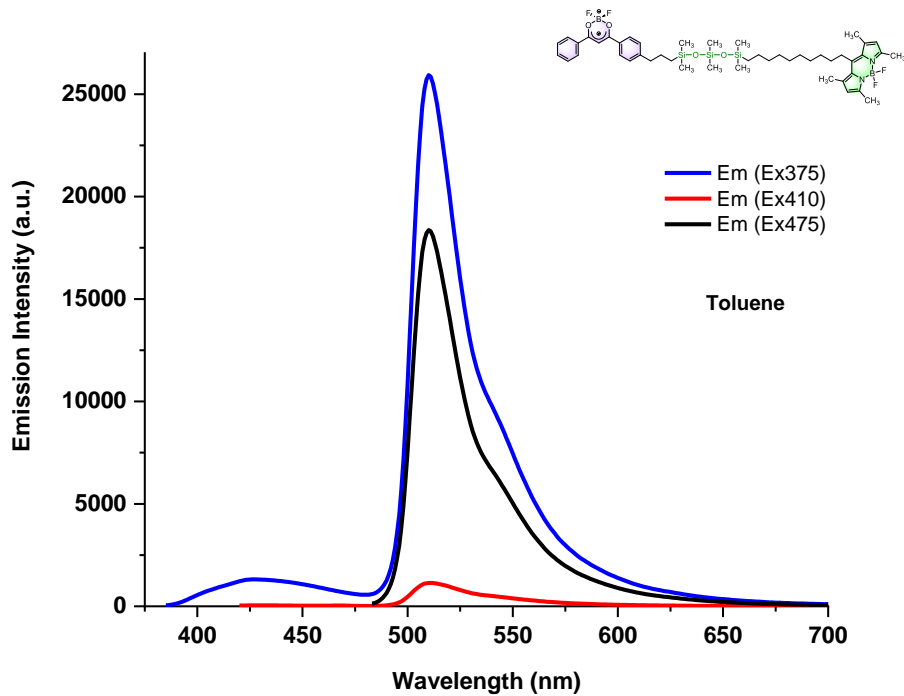

Figure S44. Emission spectra of **5 a** in toluene (c = 1 × 10^{-6} M) at different excitation wavelengths (375, 410 and 475 nm) at room temperature.
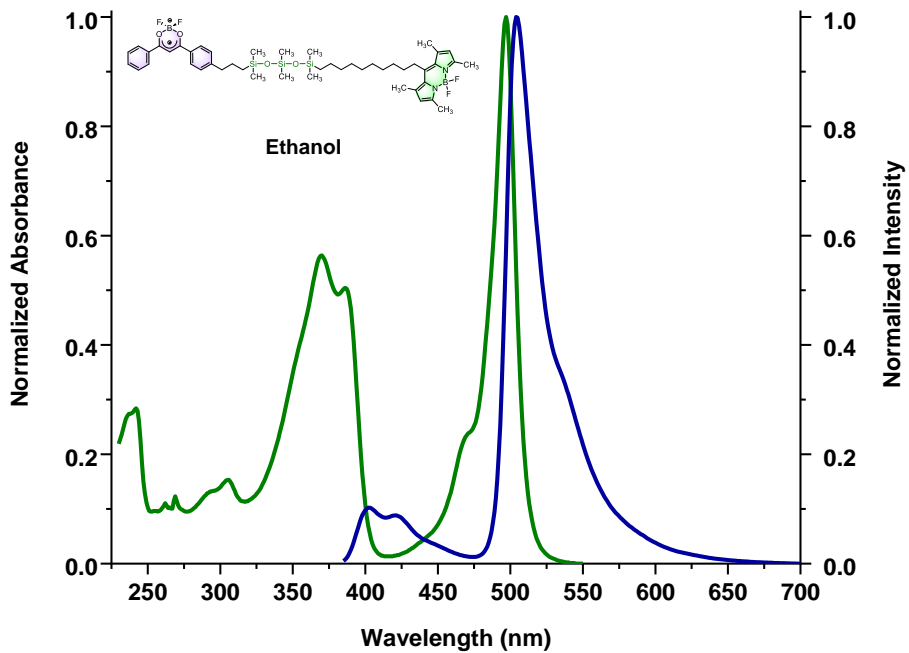
**Figure S45.** Normalized UV-visible absorption and emission spectra of **5 a** in ethanol (c = 1 × 10^{-6} M) at room temperature. Excitation at 375 nm.
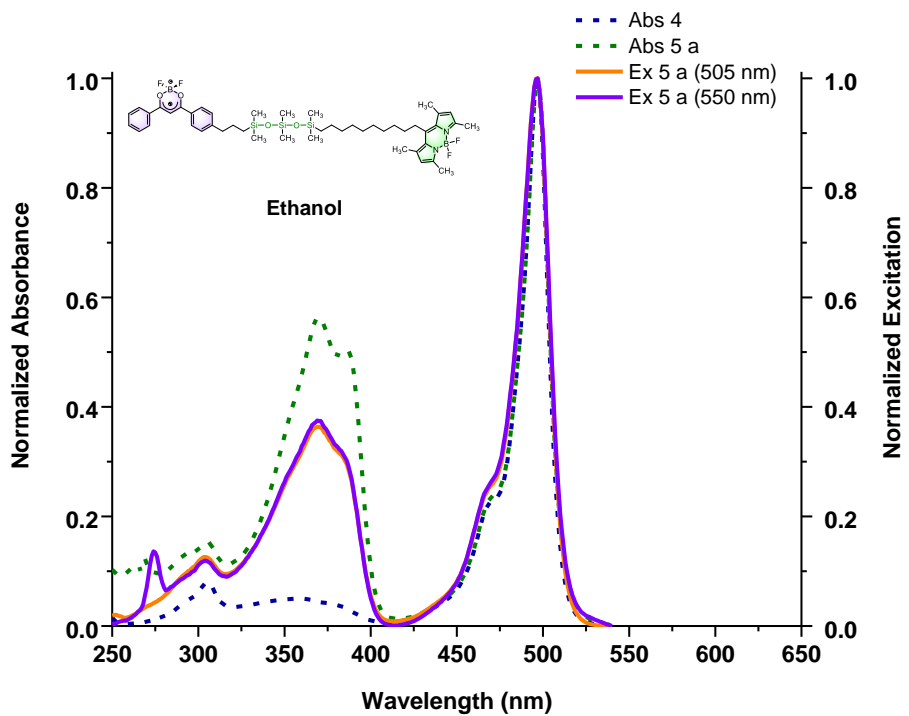

Figure S46. Normalized UV-visible absorption and excitation spectra of **5 a** in ethanol (c = 1 × 10^{-6} M) at room temperature.
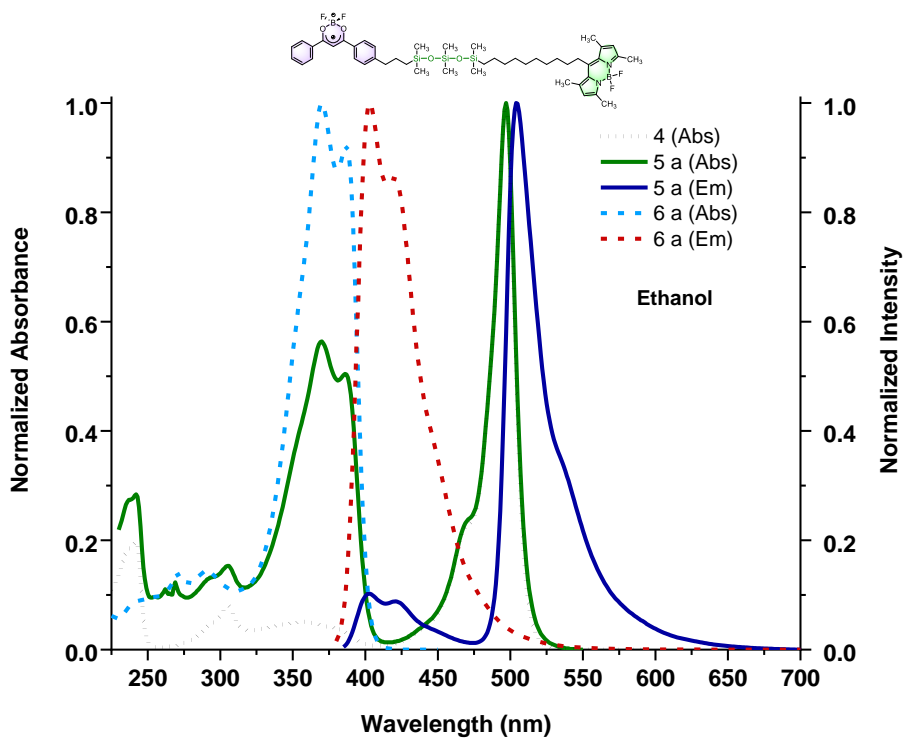
Figure S47. Normalized UV-visible absorption and emission spectra of **4**, **5 a** and **6 a** in ethanol (c = 1 × 10⁻⁶ M) at room temperature.
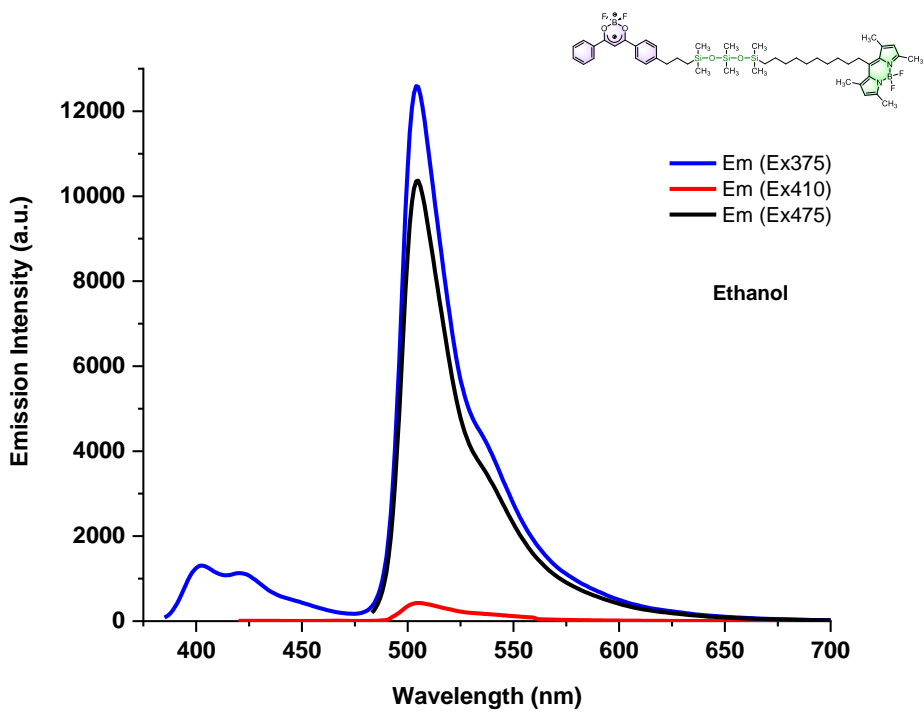
Figure S48. Emission spectra of **5 a** in ethanol (c = 1 × 10⁻⁶ M) at different excitation wavelengths (375, 410 and 475 nm) at room temperature.
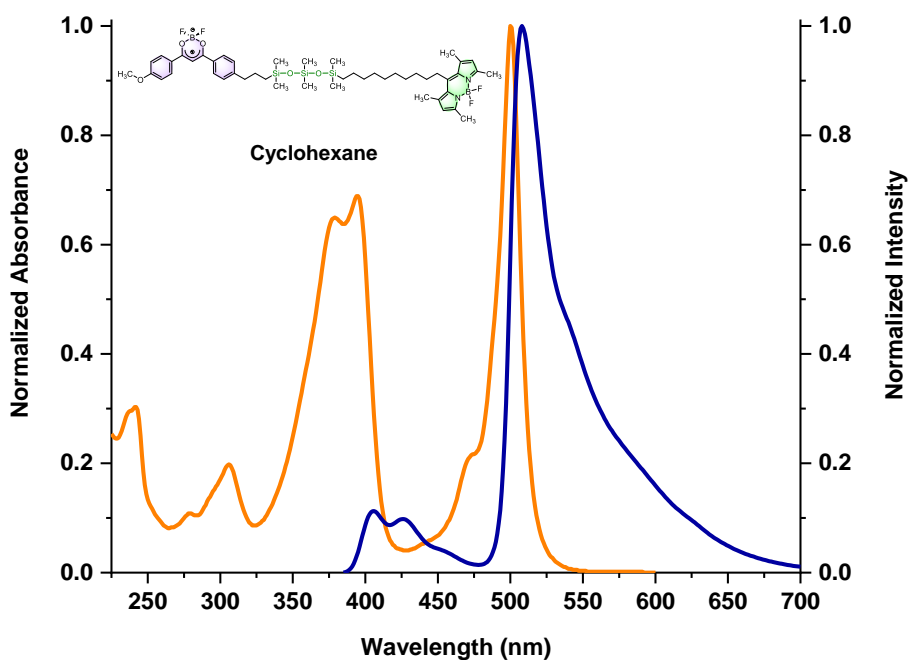
Figure S49. Normalized UV-visible absorption and emission spectra of **5 b** in cyclohexane (c = 1×10^{-6} M) at room temperature. Excitation at 375 nm.
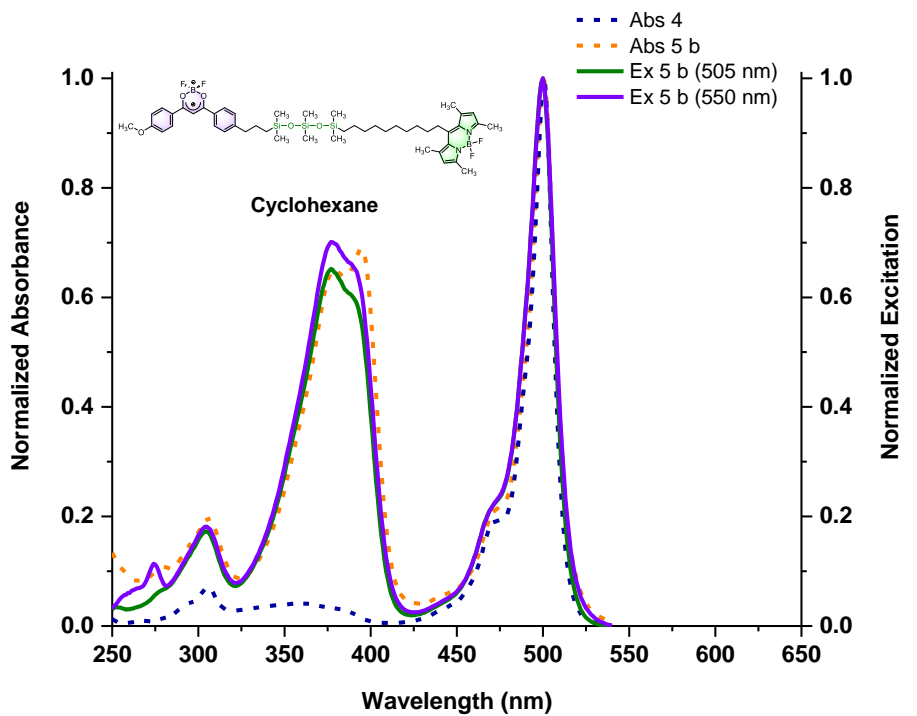

**Figure S50.** Normalized UV-visible absorption and excitation spectra of **5 b** in cyclohexane (c = 1×10^{-6} M) at room temperature.
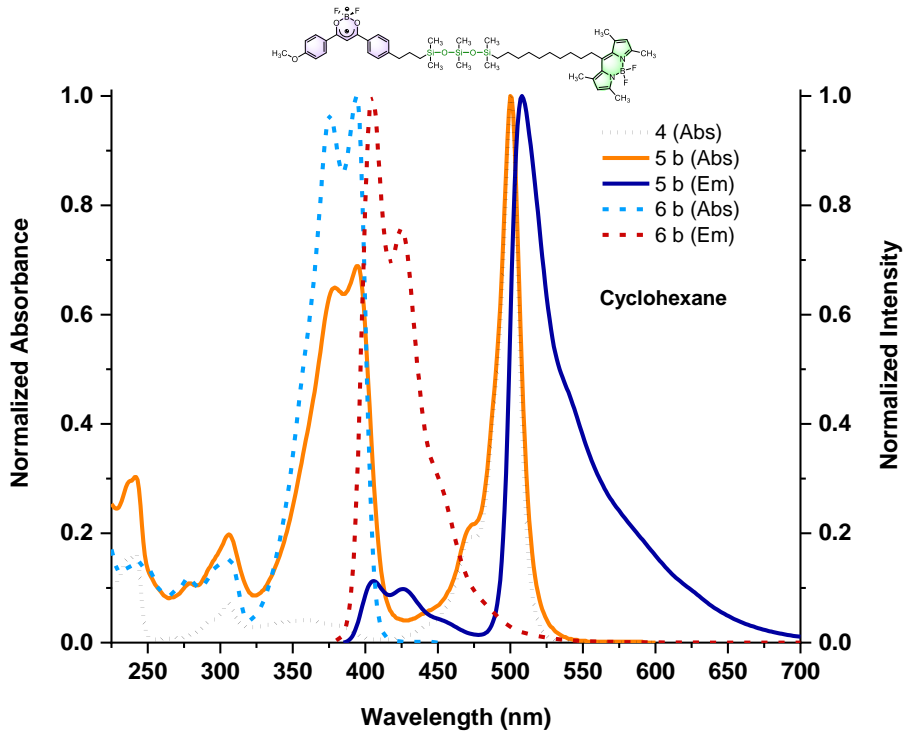
Figure S51. Normalized UV-visible absorption and emission spectra of **4**, **5 b** and **6 b** in cyclohexane (c = 1 × 10⁻⁶ M) at room temperature.
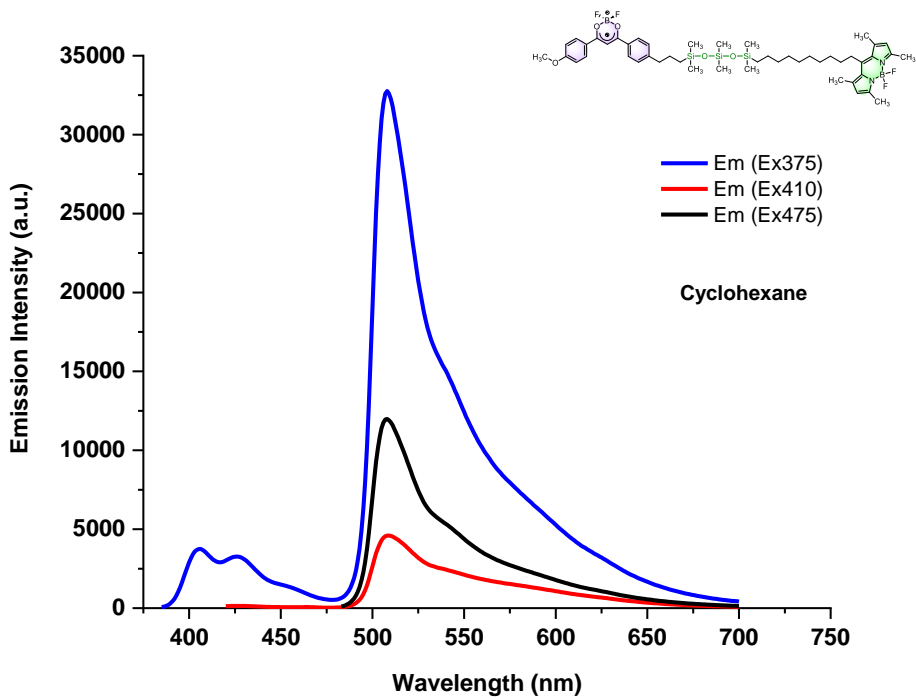
Figure S52. Emission spectra of **5 b** in cyclohexane (c = 1 × 10⁻⁶ M) at different excitation wavelengths (375, 410 and 475 nm) at room temperature.
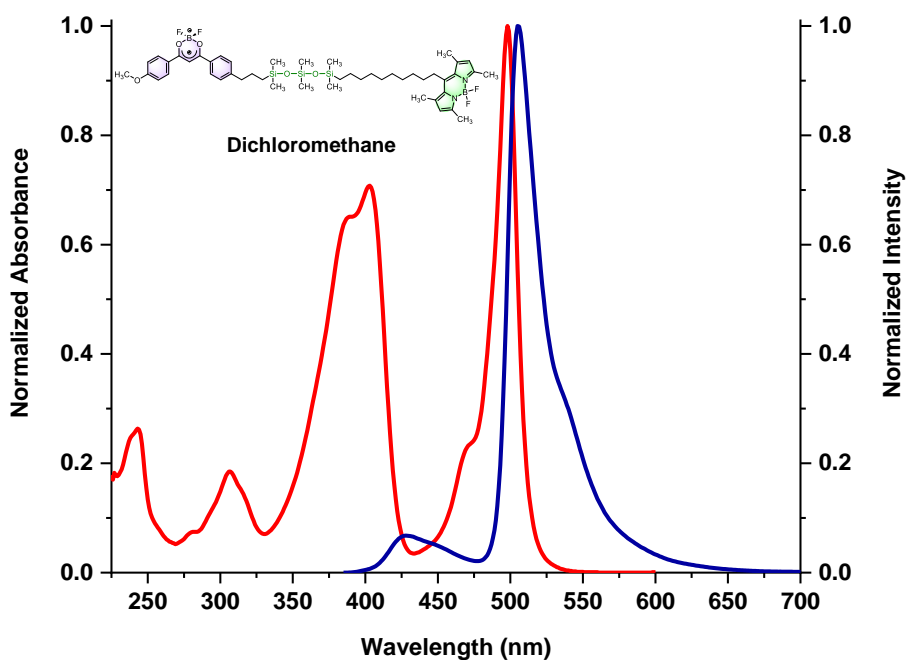
Figure S53. Normalized UV-visible absorption and emission spectra of **5 b** in dichloromethane (c = 1 × 10⁻⁶ M) at room temperature. Excitation at 375 nm.
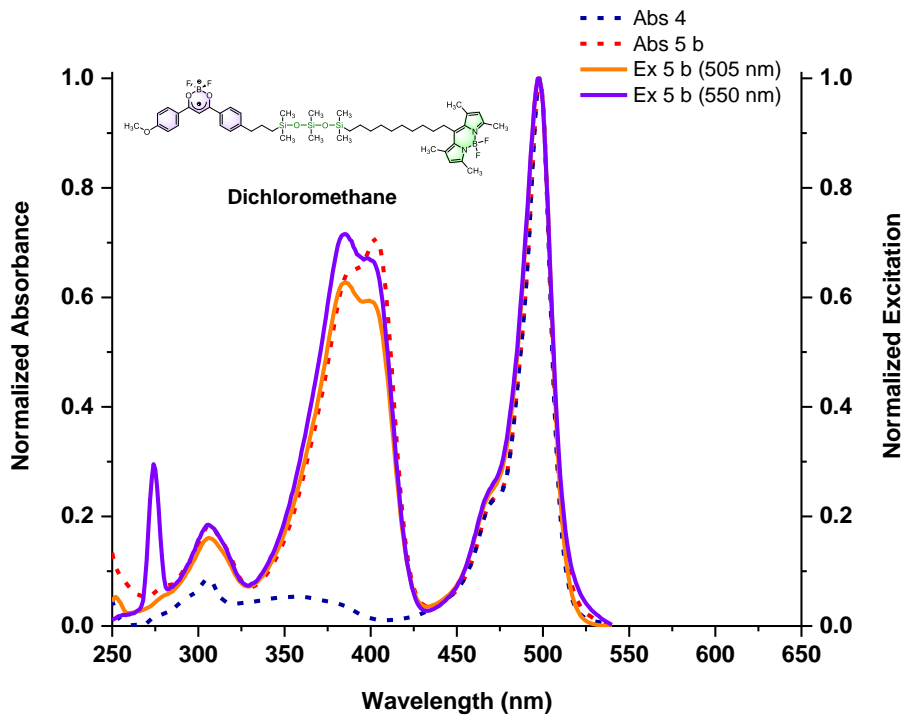
Figure S54. Normalized UV-visible absorption and excitation spectra of **5 b** in dichloromethane (c = 1 × 10⁻⁶ M) at room temperature.
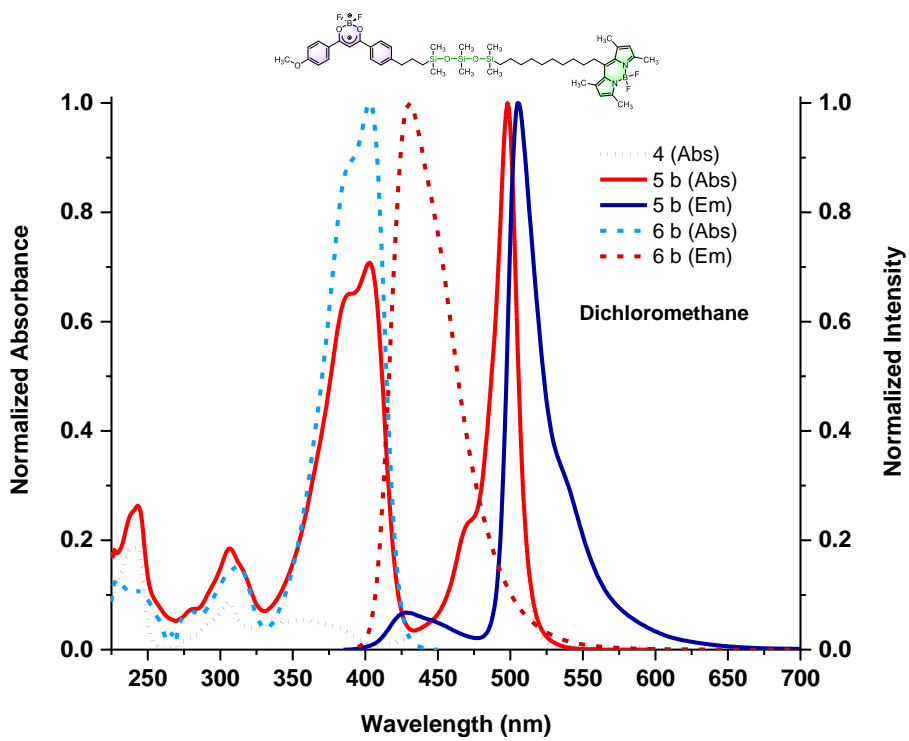
Figure S55. Normalized UV-visible absorption and emission spectra of **4**, **5 b** and **6 b** in dichloromethane (c = 1 × 10⁻⁶ M) at room temperature.
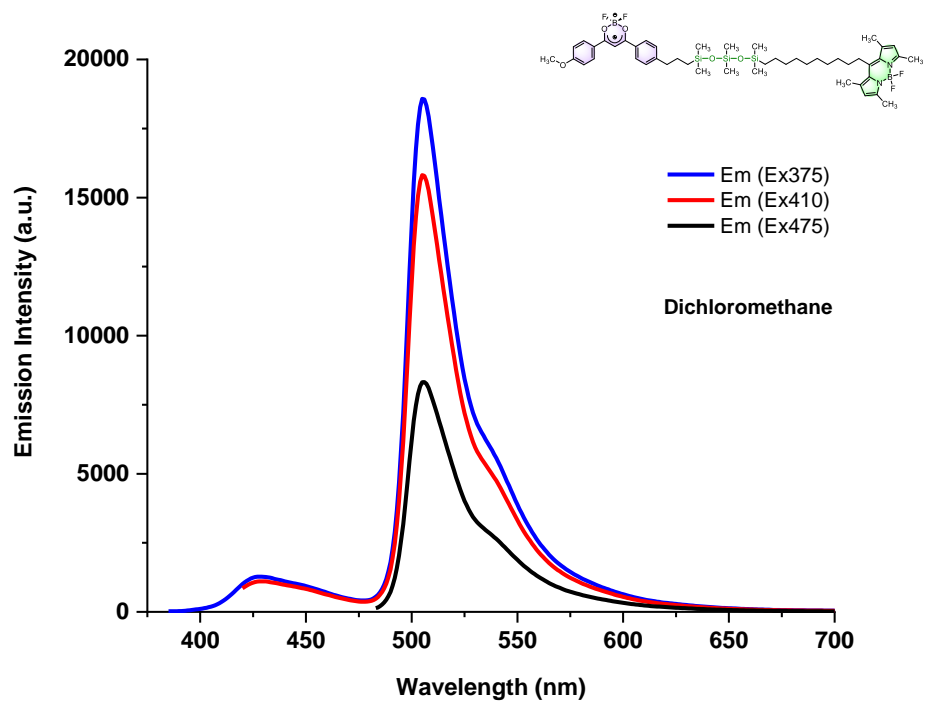

Figure S56. Emission spectra of **5 b** in dichloromethane (c = 1 × 10⁻⁶ M) at different excitation wavelengths (375, 410 and 475 nm) at room temperature.
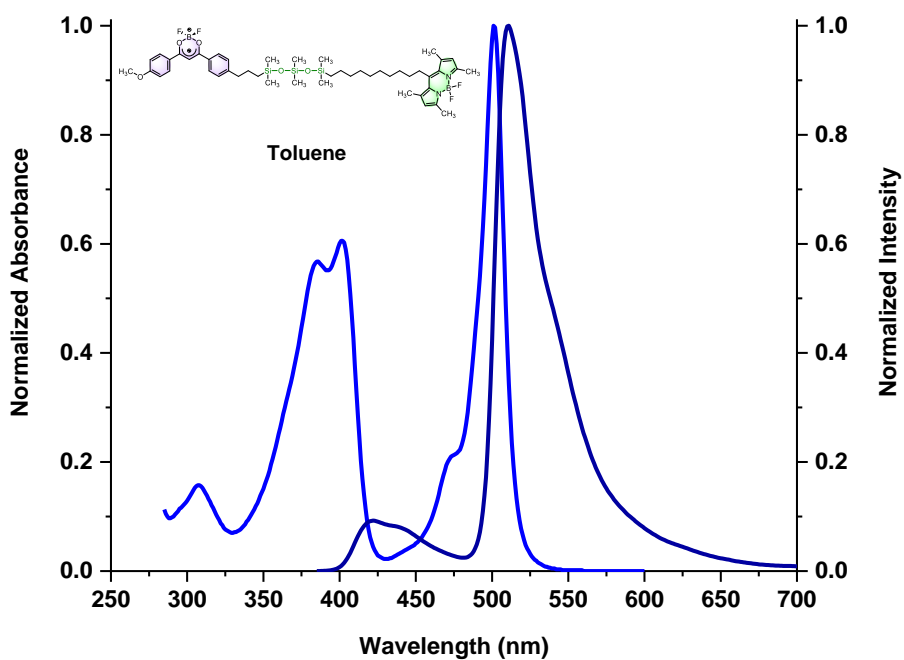
Figure S57. Normalized UV-visible absorption and emission spectra of **5 b** in toluene (c = 1 × 10⁻⁶ M) at room temperature. Excitation at 375 nm.
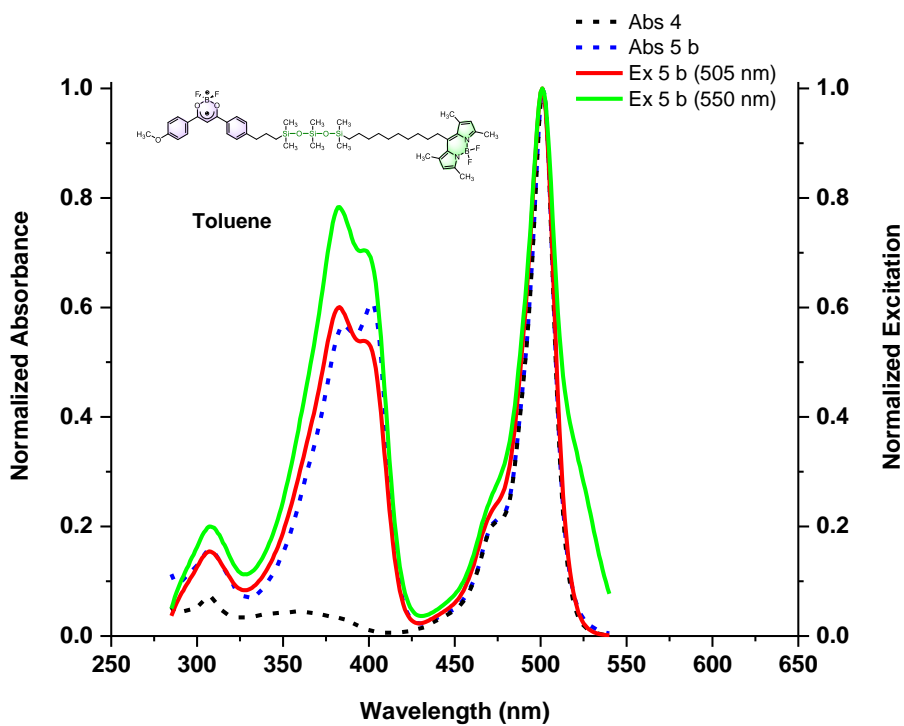

Figure S58. Normalized UV-visible absorption and excitation spectra of **5 b** in toluene (c = 1 × 10⁻⁶ M) at room temperature.
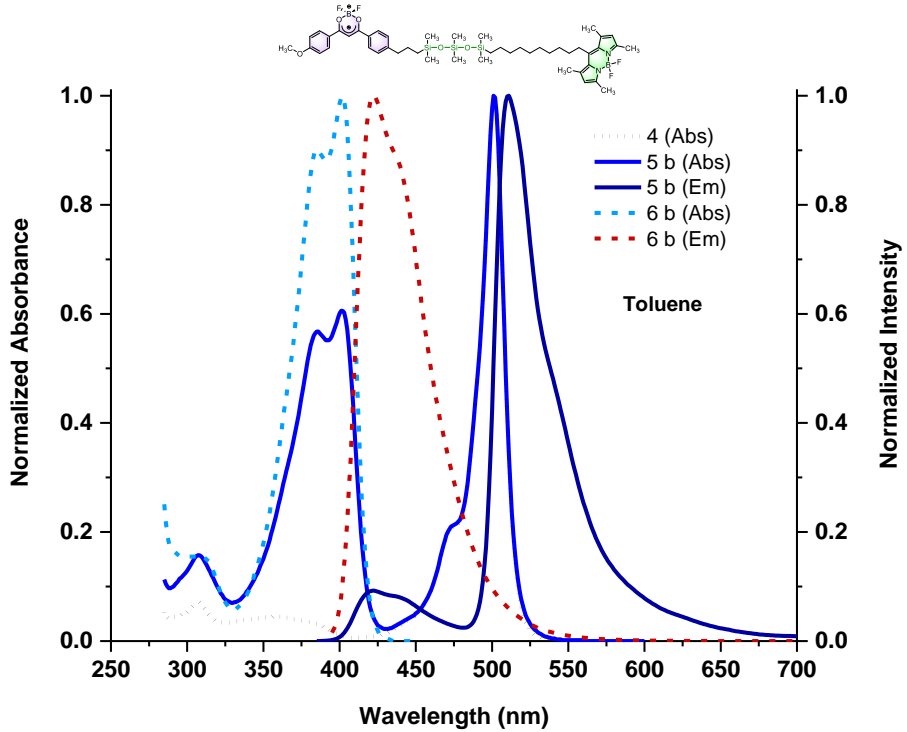
Figure S59. Normalized UV-visible absorption and emission spectra of **4**, **5 b** and **6 b** in toluene (c = 1 × 10^{-6} M) at room temperature.
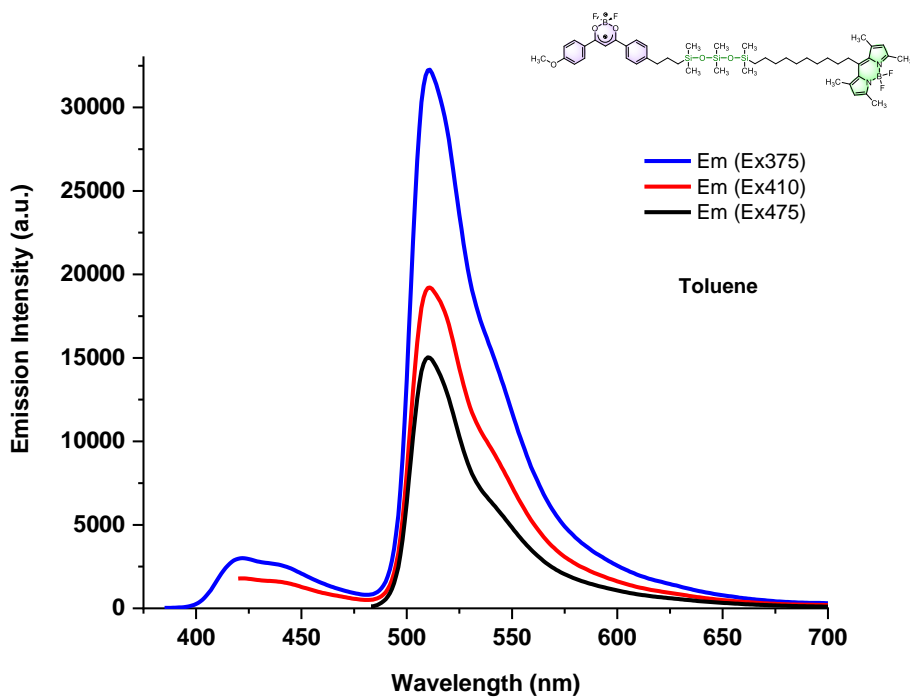

Figure S60. Emission spectra of **5 b** in toluene (c = 1 × 10^{-6} M) at different excitation wavelengths (375, 410 and 475 nm) at room temperature.
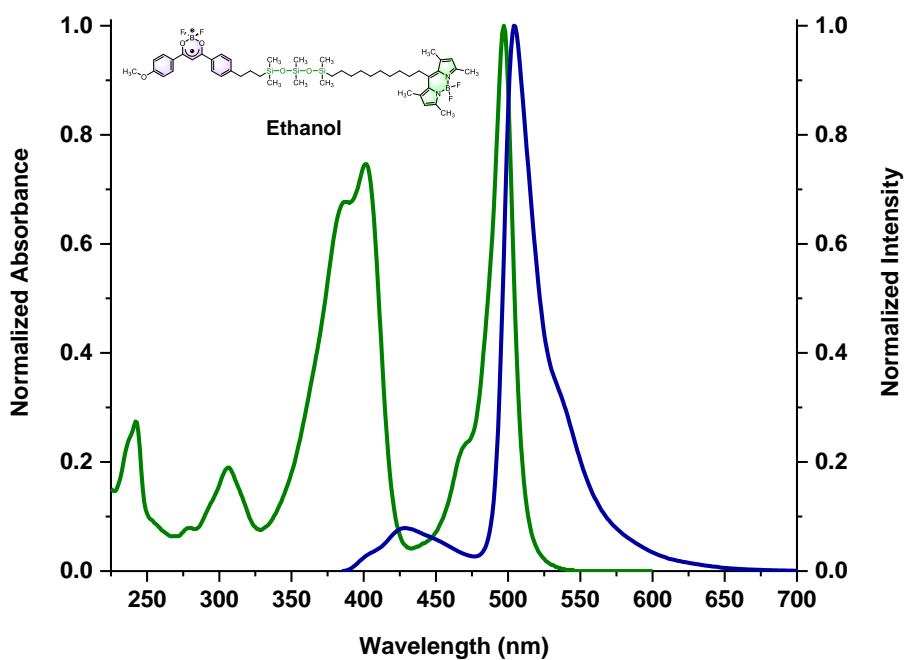
Figure S61. Normalized UV-visible absorption and emission spectra of **5 b** in ethanol (c = 1 × 10^{-6} M) at room temperature. Excitation at 375 nm.
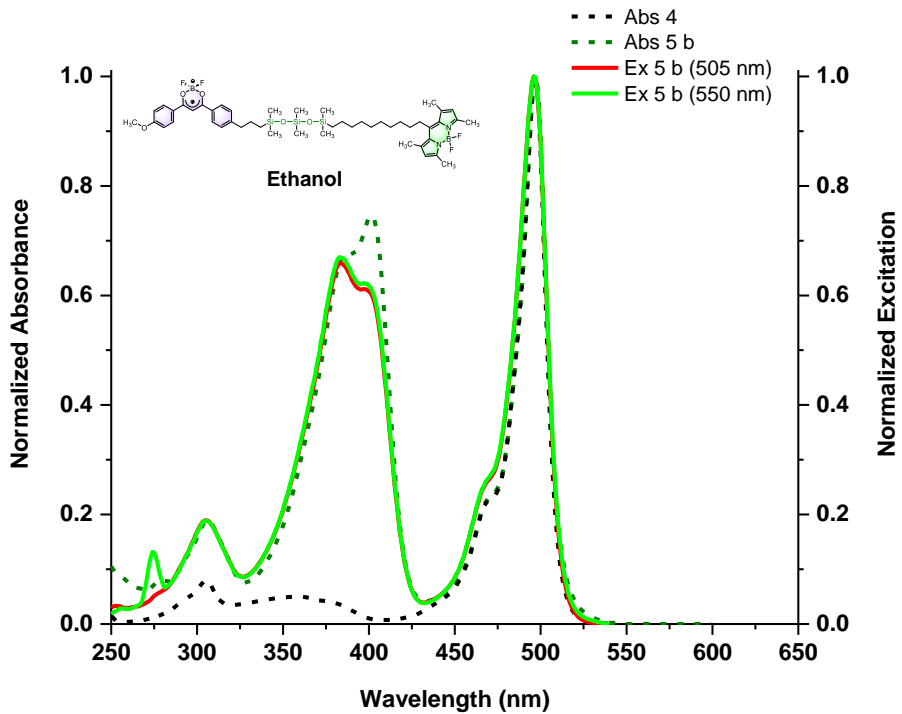

Figure S62. Normalized UV-visible absorption and excitation spectra of **5 b** in ethanol (c = 1 × 10^{-6} M) at room temperature.
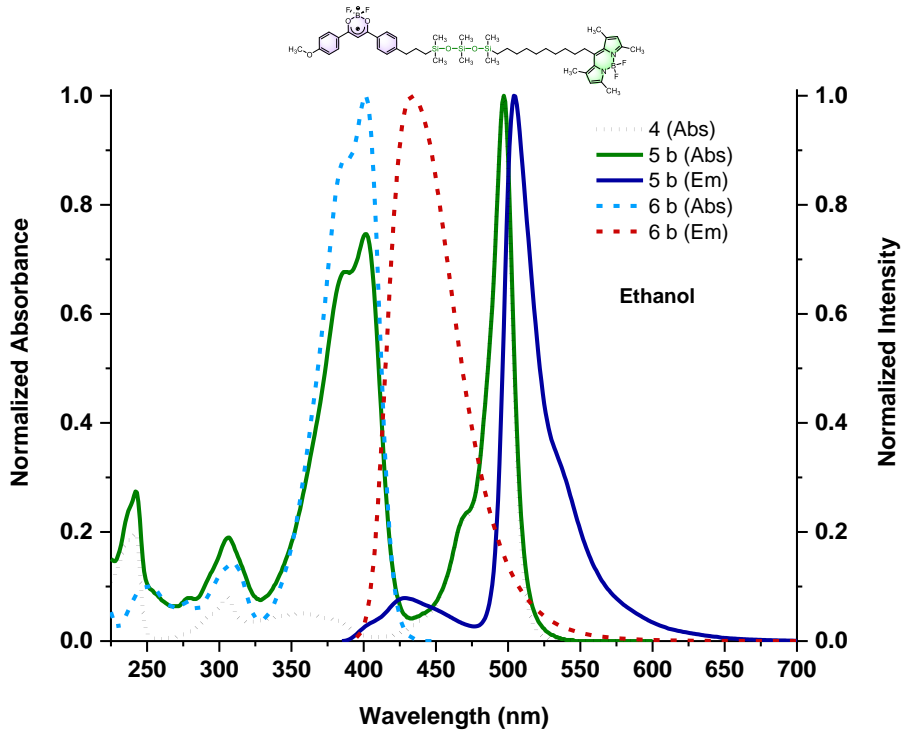
Figure S63. Normalized UV-visible absorption and emission spectra of **4**, **5 b** and **6 b** in ethanol (c = 1 × 10^{-6} M) at room temperature.
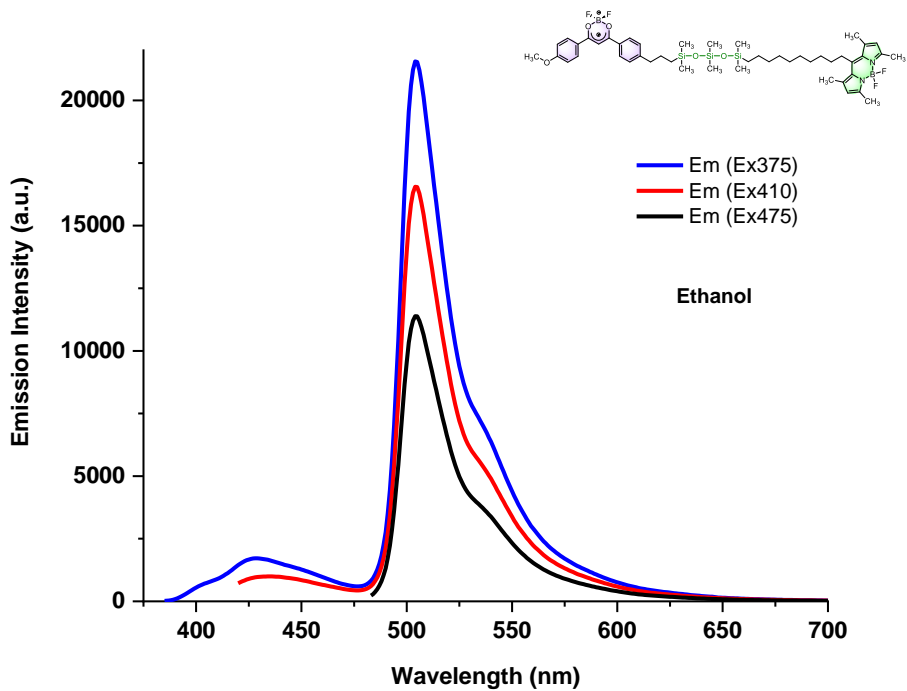

Figure S64. Emission spectra of **5 b** in ethanol (c = 1 × 10^{-6} M) at different excitation wavelengths (375, 410 and 475 nm) at room temperature.
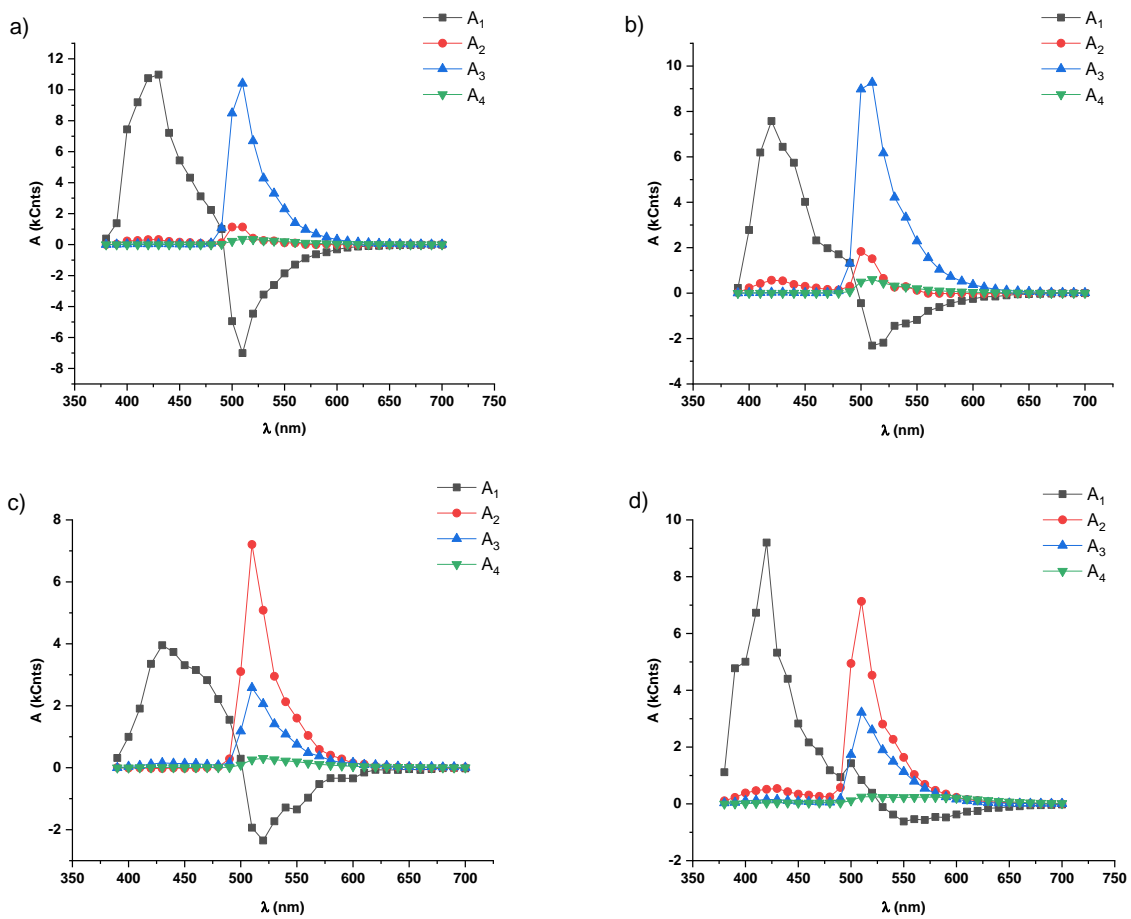
Figure S65. Amplitudes of exponential terms $A_1 - A_4$ with corresponding lifetimes $\tau_1 - \tau_4$ obtained from four exponential global fitting of fluorescence decays obtained fot **5 a** in the range of 380-700 nm with step of 10 nm (λ_{exc} = 375 nm) in (a) – dichloromethane; (b) – ethanol; (c) – toluene; (d) – cyclohexane.

Figure S66. Amplitudes of exponential terms $A_1 - A_4$ with corresponding lifetimes $\tau_1 - \tau_4$ obtained from four exponential global fitting of fluorescence decays obtained for **5 b** in the range of 380-700 nm with step of 10 nm (λ_{exc} = 375 nm) in (a) – dichloromethane; (b) – ethanol; (c) – toluene; (d) – cyclohexane.
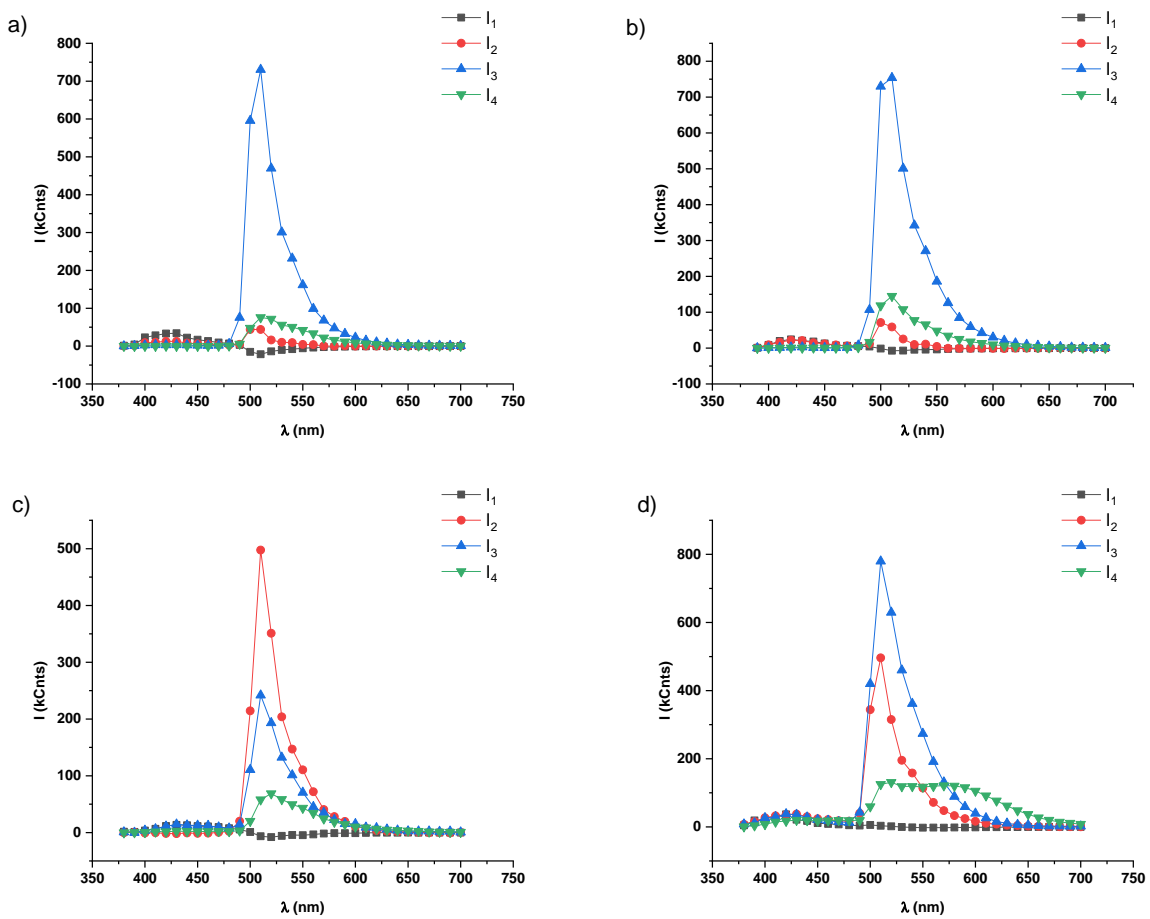
Figure S67. Fraction of intensity in steady state spectra $I_1 – I_4$ with corresponding lifetimes $\tau_1 - \tau_4$ obtained from four exponential global fitting of fluorescence decays obtained for **5 a** in the range of 380-700 nm with step of 10 nm (λ_{exc} = 375 nm) in (a) – dichloromethane; (b) – ethanol; (c) – toluene; (d) – cyclohexane.
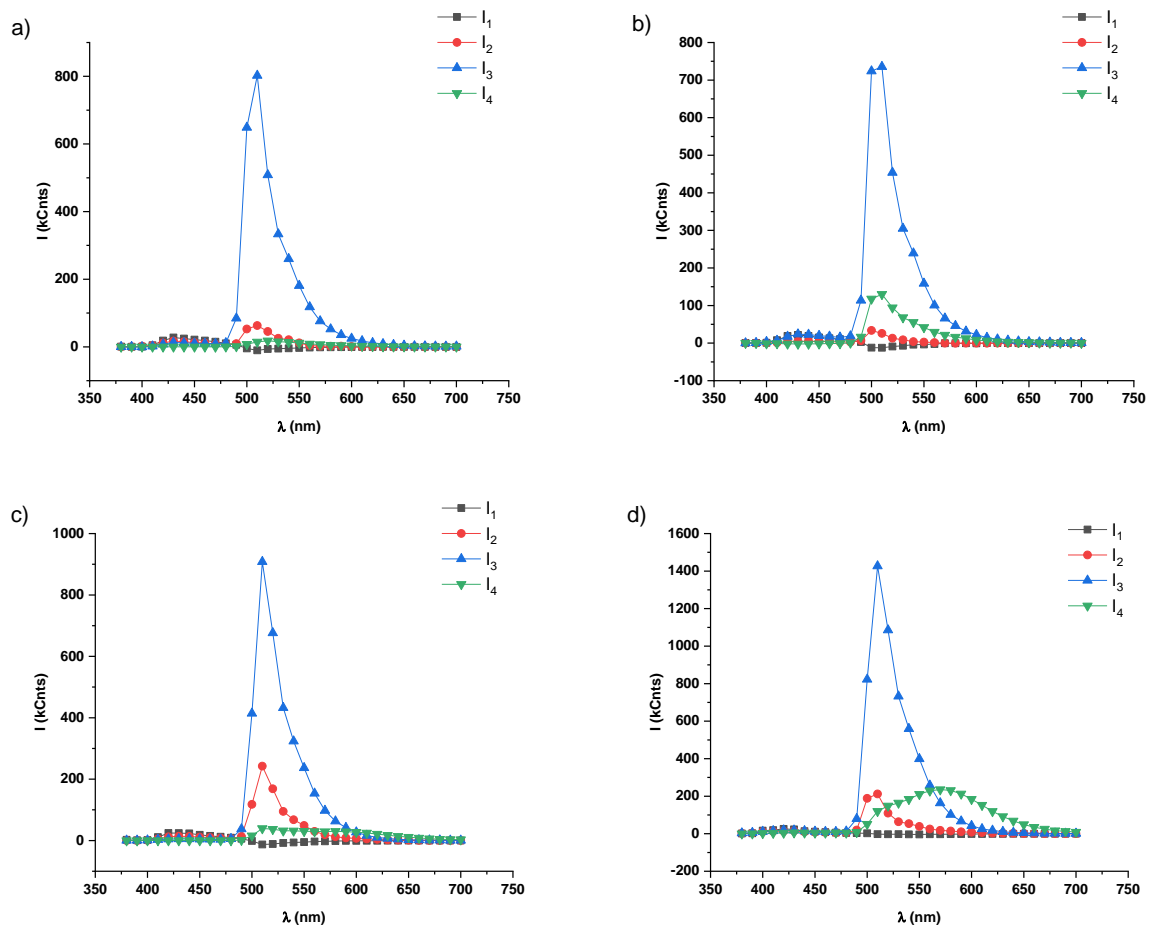
Figure S68. Fraction of intensity in steady state spectra $I_1 - I_4$ with corresponding lifetimes $\tau_1 - \tau_4$ obtained from four exponential global fitting of fluorescence decays obtained for **5 b** in the range of 380-700 nm with step of 10 nm (λ_{exc} = 375 nm) in (a) – dichloromethane; (b) – ethanol; (c) – toluene; (d) – cyclohexane.
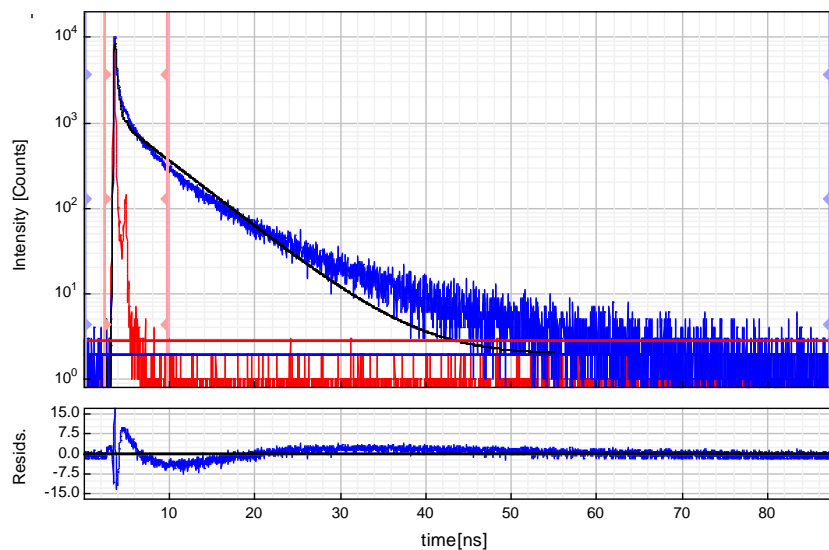
a)
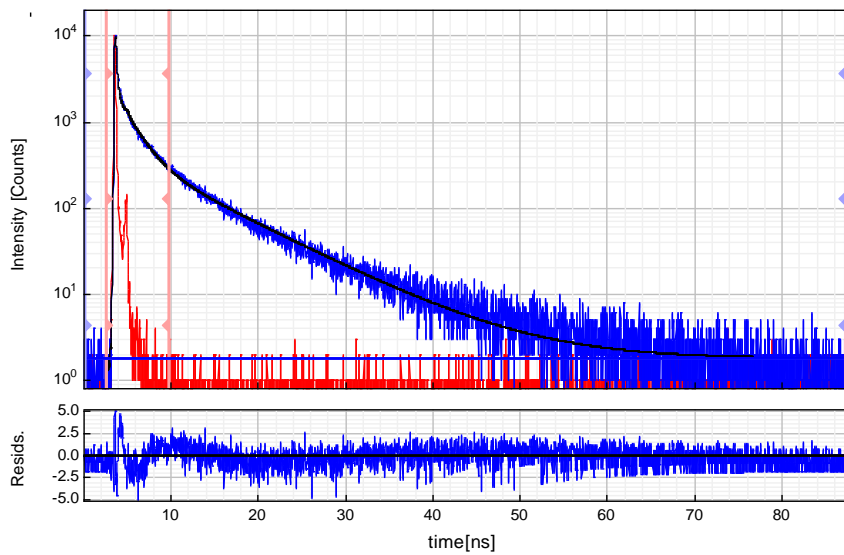
b)
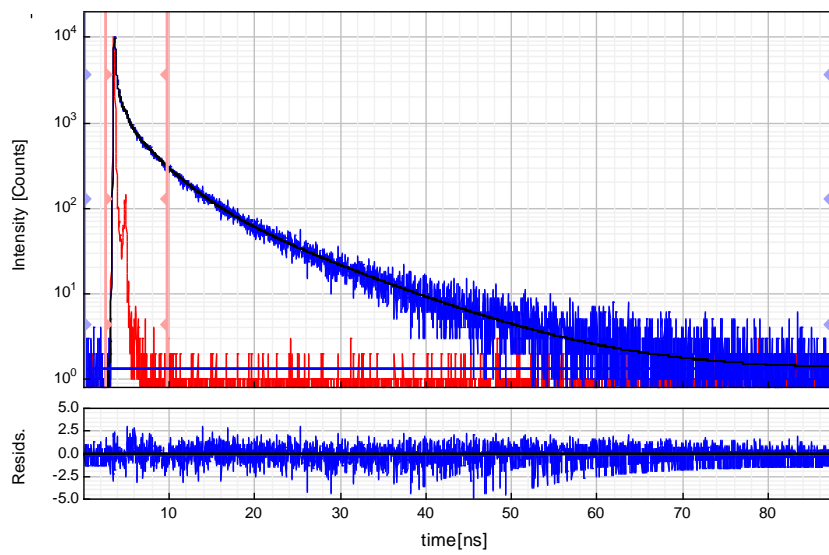

c)

Figure S69. Comparison of (a) - biexponential χ^2=4.69, (b) – triexponential χ^2=1.42 and (c) - four exponential χ^2=1.1 fitting of decay curve obtained in for **5 a** in cyclohexane (λ_{exc} = 375 nm).
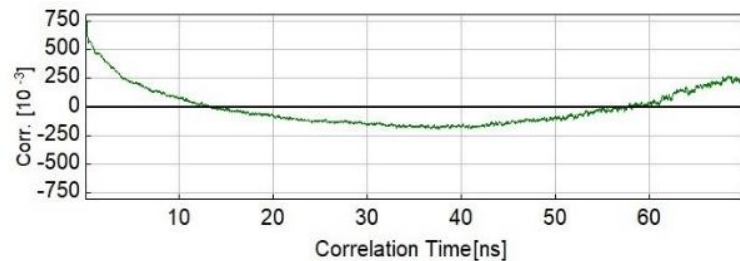
a)
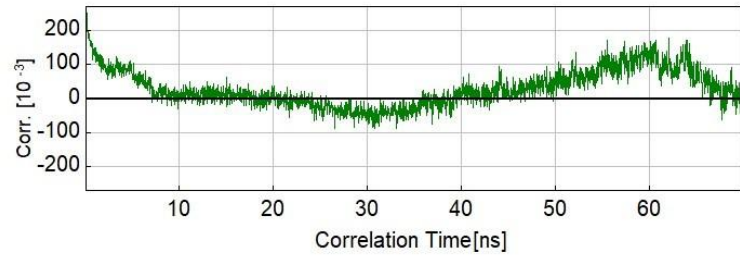
b)
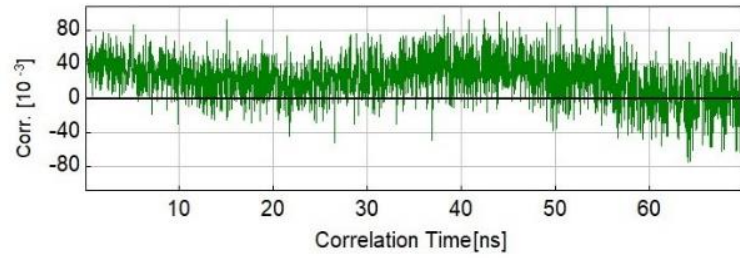
c)

Figure S70. Comparison of autocorrelation functions of (a) - biexponential χ^2=4.69, (b) – triexponential χ^2=1.42 and (c) - four exponential χ^2=1.116 fitting of decay curve obtained in for **5 a** in cyclohexane (λ_{exc} = 375 nm).

5. References

[1]   M. A. West, in *Photochemistry* (Ed.: D. Bryce-Smith), Royal Society Of Chemistry, Cambridge, **1979**, pp. 3–116.

[2]   D. O'Connor, D. Phillips, *Time-Correlated Single Photon Counting*, Elsevier, London, **1984**.

[3]   D. F. Eaton, *Pure Appl. Chem.* **1990**, *62*, 1631–1648.

[4]   B. Valeur, M. N. Berberan-Santos, in *Mol. Fluoresc.*, John Wiley & Sons, Ltd, **2012**, pp. 213–261.

[5]   D. S. Ionov, G. A. Yurasik, Y. N. Kononevich, N. M. Surin, E. A. Svidchenko, V. A. Sazhnikov, A. M. Muzafarov, M. V. Alfimov, *Nanotechnologies Russ.* **2017**, *12*, 338–351.

[6]   Y. N. Kononevich, A. S. Belova, V. A. Sazhnikov, A. A. Safonov, D. S. Ionov, A. D. Volodin, A. A. Korlyukov, A. M. Muzafarov, *Tetrahedron Lett.* **2020**, *61*, 152176.

[7]   A. A. Pakhomov, V. B. Mironiuk, Y. N. Kononevich, A. A. Korlyukov, A. D. Volodin, T. A. Pryakhina, V. I. Martynov, A. M. Muzafarov, *Mendeleev Commun.* **2017**, *27*, 363–365.